Advances in Bioresearch
Adv. Biores., Vol 17 (4) April 2026: 198-224

Print ISSN 0976-4585; Online ISSN 2277-1573
Journal's URL:http://www.soeagra.com/abr.html
CODEN: ABRDC3
DOI: 10.15515/abr.0976-4585.17.4.198224

Advances in Bioresearch

ORIGINAL ARTICLE

Phytochemical Characterization and Antidiabetic Evaluation of *Rhynchosia Rothii* using LC–HRMS and *In Silico* Approaches

Arfin S. Tamboli[1]*, Sharad D. Tayade[2], Inzamamul Haq Ameer Shaikh[1], Kedar Kailas Ganjare[1], Vijay S. Borkar[3], Jyoti Bhushan Khedekar[4]**

[*1] Research Scholar, Department of Industrial Pharmacy, Shri Sant Gajanan Maharaj College of Pharmacy, Buldana-443001, Maharashtra, India

[**2] Department of Industrial Pharmacy, Shri Sant Gajanan Maharaj College of Pharmacy, Buldana-443001, Maharashtra, India

[3] Department of Pharmaceutical Chemistry, Shri Sant Gajanan Maharaj College of Pharmacy, Buldana-443001, Maharashtra, India

[4] Department of Pharmaceutics, Shri Sant Gajanan Maharaj College of Pharmacy, Buldana-443001, Maharashtra, India

***Correspondence author email:** tamboliarfin@gmail.com; sharad_tayade1@rediffmail.com

ABSTRACT

The present study investigated the phytochemical composition and antidiabetic potential of the ethyl acetate fraction of Rhynchosia rothii. Soxhlet extraction yielded 9.9% (w/w) extract, and physicochemical evaluation confirmed its quality (pH 5.2–6.3, moisture content 6.9%, total ash 8.2%). Microbial analysis confirmed the absence of pathogenic contamination. Phytochemical screening revealed abundant flavonoids (+++), phenolics (+++), and carbohydrates (+++), indicating a polyphenol-rich profile. LC–HRMS analysis identified key bioactive compounds, including epigallocatechin (m/z 325.1, RT 1.49 min), biochanin A (m/z 284.1, RT 10.08 min), rutin (m/z 593.4, RT 13.56 min), and genistein (m/z 302.2, RT 17.91 min). Molecular docking against α-glucosidase (PDB ID: 7JTY) showed that rutin (−8.4 kcal/mol) and daidzin (−8.2 kcal/mol) exhibited higher binding affinity than the native ligand (−6.4 kcal/mol), with key interactions involving ASP305, ASP640, and TRP525. ADMET analysis indicated improved drug-likeness for compounds such as medicarpin (QED 0.865) compared to native ligand *(0.313). Absorption studies showed higher intestinal absorption for caffeic acid (HIA ~0.30), while glycosides exhibited lower permeability.* Native ligand *demonstrated low plasma protein binding (42.18%) compared to >90% for several phytoconstituents. Toxicity assessment revealed low hepatotoxicity for* native ligand *(DILI 0.029) and favorable safety for phenolic acids, whereas rutin and genistin showed higher DILI values (>0.93). Overall, Rhynchosia rothii exhibits significant antidiabetic potential, supported by strong binding affinity and favorable pharmacokinetic properties, highlighting its promise as a source of novel therapeutic agents.*

KEYWORDS: *Rhynchosia rothii*; LC–HRMS; Phytochemical profiling; α-Glucosidase inhibition; Molecular docking; ADMET analysis; Antidiabetic activity; Type 2 diabetes mellitus

Received 21.01.2026 Revised 01.03.2026 Accepted 11.04.2026

How to cite this article:
Arfin S. T, Sharad D. T, Inzamamul Haq A S, Kedar Kailas G, Vijay S. B, Jyoti Bhushan K. Phytochemical Characterization and Antidiabetic Evaluation of *Rhynchosia Rothii* using LC–HRMS and *In Silico* Approaches. Adv. Biores. Vol 17 [4] April 2026. 198-224

INTRODUCTION

Rhynchosia rothii is a medicinal plant belonging to the Fabaceae family, widely distributed in tropical and subtropical regions and traditionally used in various indigenous systems of medicine. Plants of this genus are known to be rich sources of bioactive phytoconstituents, including flavonoids, isoflavonoids, phenolic acids, and glycosides, which are associated with diverse pharmacological activities. These secondary metabolites play a significant role in plant defense mechanisms and have been extensively explored for their therapeutic potential, particularly in managing chronic diseases. The growing interest in plant-derived compounds has encouraged scientific validation of traditionally used plants, including *Rhynchosia rothii*, for their pharmacological efficacy [1–3].

Type 2 diabetes mellitus (T2DM) is a chronic metabolic disorder characterized by insulin resistance, impaired insulin secretion, and persistent hyperglycemia. The global prevalence of T2DM has increased dramatically due to sedentary lifestyles, dietary changes, and genetic predisposition, making it a major public health concern. One of the key therapeutic strategies for managing postprandial hyperglycemia involves the inhibition of carbohydrate-hydrolyzing enzymes such as α-glucosidase, which delays glucose absorption in the intestine. Although synthetic inhibitors are available, their long-term use is often associated with adverse effects, necessitating the search for safer and more effective alternatives from natural sources [4–6].

Natural products, particularly those derived from medicinal plants, offer a promising approach for the development of novel antidiabetic agents due to their structural diversity and biological compatibility. Flavonoids and phenolic compounds have been widely reported to exhibit α-glucosidase inhibitory activity along with antioxidant and anti-inflammatory properties. The extraction of such bioactive compounds using appropriate solvents is a critical step in maximizing their yield and activity [7–9]. Ethyl acetate is commonly employed as a semi-polar solvent for extracting flavonoids and related compounds, providing fractions enriched with pharmacologically active constituents.

Advanced analytical techniques such as Liquid Chromatography–High Resolution Mass Spectrometry (LC–HRMS) enable comprehensive profiling and identification of phytoconstituents with high sensitivity and accuracy [10–12]. In addition, computational approaches such as molecular docking facilitate the prediction of interactions between bioactive compounds and target proteins, providing insights into their mechanism of action. Furthermore, ADMET (Absorption, Distribution, Metabolism, Excretion, and Toxicity) analysis aids in evaluating the pharmacokinetic and safety profiles of potential drug candidates at an early stage [13–15].

Therefore, the present study aims to investigate the phytochemical composition of the ethyl acetate fraction of *Rhynchosia rothii* and to evaluate its potential antidiabetic activity using LC–HRMS analysis, molecular docking, and ADMET profiling, providing a scientific basis for its potential application in the management of type 2 diabetes mellitus.

MATERIAL AND METHODS

Collection of Plant Material and Authentication

Rhynchosia rothii herb was collected in December 2025 from a local area of Buldhana, Maharashtra, India. The collected plant material was processed to prepare an herbarium specimen and authenticated by the Department of Botany, Government Degree College, Kukatpally, Medchal District, Telangana (affiliated to Osmania University). Authentication was carried out by P. Suresh Babu, and a voucher specimen (No. 0274) was deposited for future reference. The authentication certificate was issued on 26.02.2026. Following authentication, the plant material was subjected to extraction. The images of the plant are presented in Figure 1.

Figure 1: The *Rhynchosia rothii* plant collected from Buldhana District

Soxhlet Extraction using Ethyl Acetate

For extraction, *Rhynchosia rothii* leaves and bark were collected and thoroughly washed with distilled water to remove dust and foreign particles, followed by air-drying in the shade at room temperature for one week to prevent degradation of heat-sensitive and volatile phytoconstituents. Approximately 500 g of the dried plant material was coarsely powdered using a mechanical grinder. The powdered material was then subjected to Soxhlet extraction using ethyl acetate as the solvent in a Soxhlet apparatus. The extraction was carried out for approximately 24 hours to ensure exhaustive extraction of semi-polar

phytoconstituents, during which multiple siphon cycles were completed. The gradual change in solvent color to dark green in the round-bottom flask (RBF), along with the fading color of the plant material in the extraction chamber, indicated efficient extraction. After completion, the extract collected in the RBF was transferred into Petri plates and allowed to evaporate naturally at room temperature to obtain a concentrated extract [16,17]. The resulting extract was then stored and further subjected to qualitative phytochemical analysis. The working photographs of Soxhlet extraction are depicted in Figure 2.

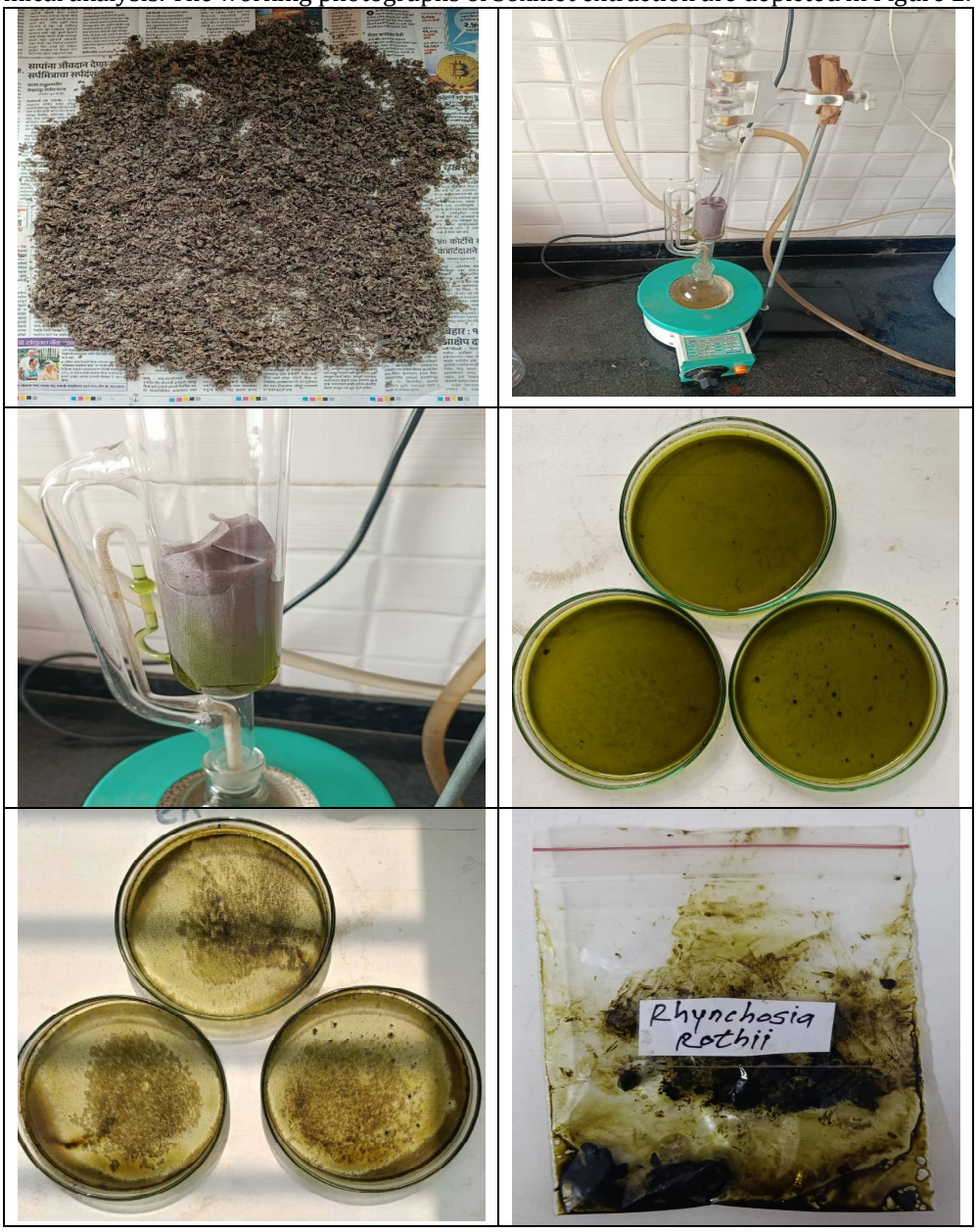

Figure 2: The Soxhlet extraction of *Rhynchosia rothii*

Physicochemical Analysis

The physicochemical evaluation of the ethyl acetate extract of *Rhynchosia rothii* was carried out to determine its quality, purity, and standardization parameters. Organoleptic properties such as colour, odour, and taste were assessed under natural light and by sensory evaluation. The pH of the extract was determined by preparing 1% and 10% aqueous solutions, and measurements were recorded using a calibrated digital pH meter. Foreign matter was evaluated by separating and weighing extraneous materials from a known quantity of the sample, and the percentage was calculated accordingly. Moisture content was determined by loss on drying (LOD) at 105 °C until a constant weight was obtained. Ash values including total ash, acid-insoluble ash, sulphated ash, and water-soluble ash were determined using standard procedures to assess inorganic content and purity of the extract. Extractive values were

determined by maceration of the sample in alcohol and water, followed by filtration and evaporation to calculate alcohol-soluble and water-soluble extractives. Heavy metal analysis was performed using atomic absorption spectrometry after acid digestion of the sample, while pesticide residues were evaluated using gas chromatography with an electron capture detector. These analyses ensured the safety and quality of the plant extract [16,18].

Qualitative Phytochemical Screening

Qualitative phytochemical screening of the ethyl acetate extract of *Rhynchosia rothii* was performed to identify major classes of bioactive constituents using standard chemical tests. The extract was subjected to specific reagents, and the formation of characteristic colour changes or precipitates indicated the presence of respective phytochemicals. Carbohydrates and reducing sugars were detected by Molisch's, Fehling's, Benedict's, and Barfoed's tests. Proteins and amino acids were evaluated using Biuret, Million's, Xanthoprotein, and Ninhydrin tests. The presence of fats and oils was confirmed by solubility and saponification tests, while steroids were identified using Salkowski and Liebermann–Burchard reactions. Cardiac glycosides were determined using Keller–Killiani and Legal's tests, whereas anthraquinone glycosides were identified by Borntrager's and modified Borntrager's tests. Saponins were confirmed by the foam test, and cyanogenetic glycosides were evaluated using sodium picrate paper. Flavonoids were detected using Shinoda, lead acetate, ferric chloride, and alkaline reagent tests. Alkaloids were confirmed by Dragendorff's, Mayer's, Wagner's, and Hager's tests. Tannins and phenolic compounds were identified using ferric chloride, lead acetate, potassium permanganate, and other confirmatory tests. This comprehensive qualitative analysis provided preliminary confirmation of diverse phytoconstituents, supporting further LC–HRMS and pharmacological studies [16,18].

Microbial Content Determination

The microbial quality of the ethyl acetate extract of *Rhynchosia rothii* was assessed by total microbial load and detection of specific pathogens using standard methods. Samples (1 g solid or 1 mL liquid) were diluted, serially diluted, and analyzed by the pour plate method. Plates were incubated at 37 °C for 24 h (bacteria) and 27 °C for 72 h (fungi), and CFU counts were recorded. Nutrient, MacConkey, Cetrimide, and Salt agar were used for bacterial enumeration, while Sabouraud dextrose agar was used for fungi.

Pathogen detection employed enrichment techniques: Escherichia coli via nutrient and MacConkey broth; Salmonella spp. using Selenite and Tetrathionate broths followed by Deoxycholate citrate agar; Shigella spp. on Salmonella–Shigella agar with TSI confirmation; Pseudomonas aeruginosa on Cetrimide agar with oxidase test; and Staphylococcus aureus on Mannitol Salt Agar with catalase and coagulase tests. These procedures ensured comprehensive microbial safety evaluation.[19,20].

LC–HRMS Analysis

The phytochemical profiling of the ethyl acetate fraction of *Rhynchosia rothii* was carried out using Liquid Chromatography–High Resolution Mass Spectrometry (LC–HRMS). The analysis was performed on an LC–HRMS system equipped with an electrospray ionization (ESI) source operating in both positive and negative ion modes. Chromatographic separation was achieved using an Accucore C18 column (150 × 4.6 mm, 2.6 µm), ensuring efficient separation of compounds with varying polarity. The sample was injected and eluted under optimized conditions, and data were acquired as base peak intensity (BPI) chromatograms over a retention time range of 0–40 min. Major peaks were observed at retention times around 1.49, 10–12, 16.52, and 24–33 min, indicating the presence of diverse phytoconstituents. Mass spectra were recorded, and compound identification was performed based on observed m/z values, fragmentation patterns, and comparison with reported literature. The LC–HRMS data were further analyzed to tentatively identify flavonoids, isoflavonoids, phenolic acids, and glycosidic derivatives present in the extract [10,21].

Molecular Docking

Molecular docking studies were performed to evaluate the binding interactions of phytoconstituents identified from LC–HRMS analysis with the target protein associated with T2DM. The three-dimensional structure of the target protein was retrieved from the Protein Data Bank using PDB ID: 7JTY. The protein structure was prepared by removing water molecules, ligands, and other heteroatoms, followed by the addition of hydrogen atoms and energy minimization using Discovery Studio [22,23]. The chemical structures of selected compounds were obtained from PubChem or drawn using ChemDraw and converted into suitable 3D formats. Energy minimization of ligands was carried out prior to docking. Molecular docking was performed using PyRx with AutoDock Vina as the docking engine. The active site of the protein was defined based on grid box coordinates (X = −10.593294, Y = 22.647882, Z = −12.077000). Docking parameters were set to default values, and binding affinities were calculated for each ligand. The docked complexes were analyzed using Discovery Studio to evaluate binding interactions such as hydrogen bonding, hydrophobic interactions, and π–π stacking. The results were used to identify

potential bioactive compounds with strong binding affinity toward the target protein for further antidiabetic investigation [22,24]. Active cavity of alpha glucosidase with native ligand are shown in Figure 3.

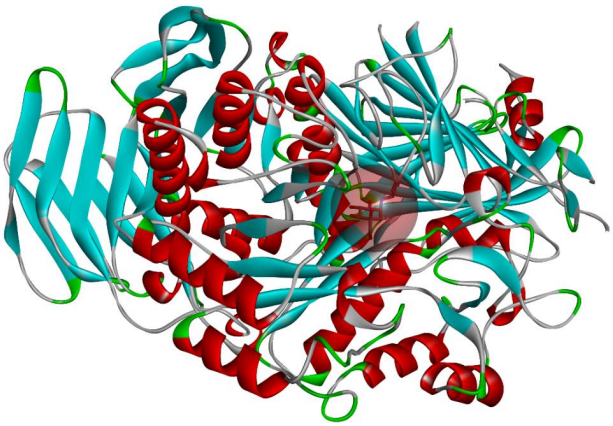

Figure 3: Active cavity of alpha glucosidase with native ligand

ADMET Analysis

ADMET (Absorption, Distribution, Metabolism, Excretion, and Toxicity) properties of phytoconstituents identified from LC-HRMS analysis were evaluated using in silico tools. Chemical structures were retrieved from PubChem or drawn using ChemDraw [25]. The structures were analyzed using SwissADME to assess physicochemical properties, lipophilicity, solubility, gastrointestinal absorption, blood–brain barrier permeability, and drug-likeness. Toxicity parameters including hepatotoxicity, mutagenicity, and carcinogenicity were predicted using ADMETlab 3.0. The results were used to identify compounds with favorable pharmacokinetic and safety profiles, supporting the selection of potential bioactive candidates for further antidiabetic evaluation [4,24].

RESULTS AND DISCUSSION

Organoleptic and Physicochemical Analysis of Extracts

The organoleptic evaluation of the ethyl acetate extract of *Rhynchosia rothii* revealed distinct sensory characteristics indicative of its phytochemical composition (Figure 4). The extract exhibited a dark green color, suggesting the presence of chlorophyll along with phenolic constituents. The characteristic, slightly aromatic odour and bitter taste indicate the presence of bioactive compounds such as flavonoids, alkaloids, and glycosides. The sticky, semi-solid texture may be attributed to the presence of sugars, resins, and other viscous phytoconstituents. The percentage yield of 9.9% (w/w) reflects efficient extraction and satisfactory recovery of semi-polar constituents. The physicochemical parameters further confirmed the quality and purity of the extract. The pH values of 6.3 (1% solution) and 5.2 (10% solution) indicate a mildly acidic nature, commonly associated with phenolic and organic acid-rich plant extracts. The low foreign content (0.5%) suggests minimal contamination and proper handling of raw material. The loss on drying (6.9%) indicates low moisture content, which is favorable for stability and reduces the risk of microbial growth. Ash values provide insight into the inorganic composition of the extract. The total ash value (8.2%) represents overall mineral content, while the acid-insoluble ash (1.8%) indicates minimal silica and earthy impurities. The water-soluble ash (3.7%) reflects the presence of soluble inorganic salts, and the sulphated ash value (8.7%) confirms total inorganic residue, suggesting low adulteration. Extractive values demonstrated that the extract is rich in bioactive constituents. The alcohol-soluble extractive (12.3%) indicates the presence of moderately polar compounds, whereas the higher water-soluble extractive (16.5%) suggests abundance of polar constituents such as tannins and phenolics. The absence of heavy metals and pesticide residues confirms the safety and purity of the extract. Overall, these findings indicate that the extract possesses good quality, stability, and suitability for further phytochemical and pharmacological investigations.

Qualitative Phytochemical Screening of Extract

The qualitative phytochemical screening of the ethyl acetate extract of *Rhynchosia rothii* revealed the presence of diverse bioactive constituents with varying intensities (Figure 5). The results indicated that carbohydrates (+++), phenolic compounds (+++), and flavonoids (+++) were abundantly present, suggesting a phytochemical profile dominated by polyphenolic constituents. The high abundance of carbohydrates, along with reducing sugars (++) and monosaccharides (++), indicates the presence of primary metabolites, which may also contribute to the formation of glycosidic secondary metabolites. The

predominance of phenolic compounds and flavonoids highlights the extract as a rich source of polyphenols, which are well known for their antioxidant, antidiabetic, and antimicrobial properties. The moderate presence of tannins (++) further supports this observation, as tannins are complex phenolic compounds associated with free radical scavenging and protective biological activities. Steroids (++) were moderately present, indicating the occurrence of phytosterols that may contribute to membrane stability and therapeutic effects. The presence of fats and oils (+) and saponin glycosides (+) in low amounts suggests minor contributions of lipophilic and glycosidic constituents. Alkaloids (+) were detected in trace amounts, indicating limited but potential pharmacological relevance. In contrast, proteins, amino acids, cardiac glycosides, and anthraquinone glycosides were absent, suggesting their negligible presence in the extract. Overall, the phytochemical profile demonstrates a predominance of polyphenolic compounds, particularly flavonoids and phenolics, supporting the therapeutic potential of *Rhynchosia rothii* for further pharmacological investigation.

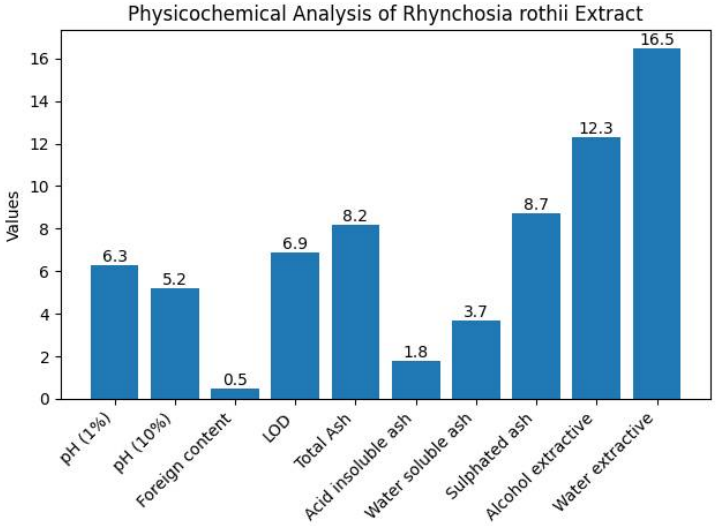

Figure 4: Physicochemical Analysis of *Rhynchosia rothii* Extract

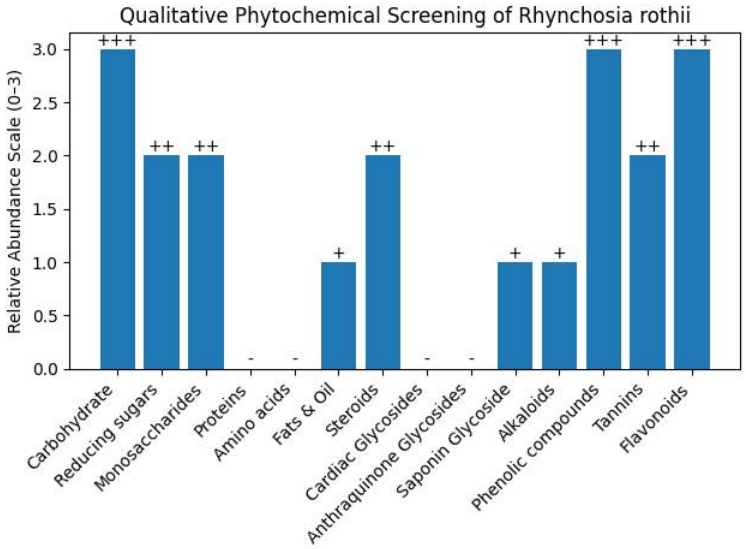

Figure 5: Qualitative physicochemical Screening of *Rhynchosia rothii*

Microbial Content Determination

The microbial analysis of the ethyl acetate extract of *Rhynchosia rothii* confirmed the absence of all tested pathogenic microorganisms, including *Escherichia coli, Salmonella spp., Shigella spp., Pseudomonas aeruginosa*, and *Staphylococcus aureus*. This indicates that the extract is free from microbial contamination and meets acceptable microbiological quality standards. The absence of enteric pathogens such as E. coli and Salmonella spp. suggests good hygienic handling, while the non-detection of P.

aeruginosa and S. aureus indicates minimal environmental and human contamination. Overall, the results demonstrate effective extraction, proper handling, and safe storage conditions, confirming that the extract is microbiologically safe and suitable for further pharmacological and formulation studies.

LC–HRMS Analysis

The LC–HRMS analysis of the ethyl acetate fraction of *Rhynchosia rothii* revealed a diverse phytochemical profile comprising flavonoids, isoflavonoids, phenolic acids, and glycosidic derivatives. The base peak chromatogram showed major peaks at retention times ~1.49, 10–12, 16.52, and 24–33 min, indicating compounds with a wide polarity range. Early eluting peaks at RT 1.49 and 1.75 min (m/z 325.1) were identified as epigallocatechin and gallocatechin, confirmed by characteristic fragment ions (m/z 145, 163), indicating highly polar flavan-3-ols. In the mid-retention region (RT 10–12 min), key isoflavonoids such as biochanin A (m/z 284.1), formononetin, calycosin, and prunetin (m/z 314.1) were detected along with phenolic acids like caffeic acid (m/z 179.1) and ferulic acid (m/z 195.1), supported by diagnostic fragmentation patterns. Glycosylated compounds including daidzin and genistin (m/z 346.2), rutin (m/z 593.4), and quercetin-3-O-glucoside (m/z 431.3) were observed between RT 12–15 min, showing characteristic sugar loss fragmentation. A prominent peak at RT 16.52 min (m/z 445.2) corresponded to kaempferol-3-O-rhamnoside, indicating a major constituent. Later retention times (RT 17–18 min) revealed aglycones such as medicarpin (m/z 332.2), daidzein, and genistein (m/z 302.2), reflecting lower polarity. Overall, the LC–HRMS data confirm a rich presence of polyphenolic compounds with potential antidiabetic activity. The LC-HRMS Analysis Graph are shown in Figure 6. LC–MS-based tentative identification of phytoconstituents with corresponding retention times are shown in Table 1.

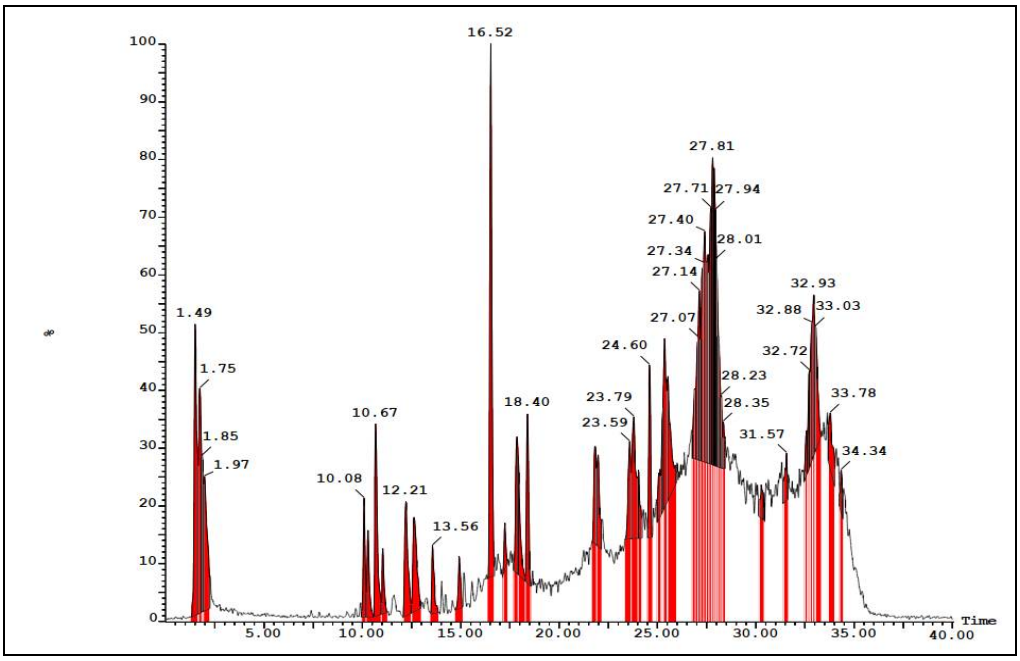

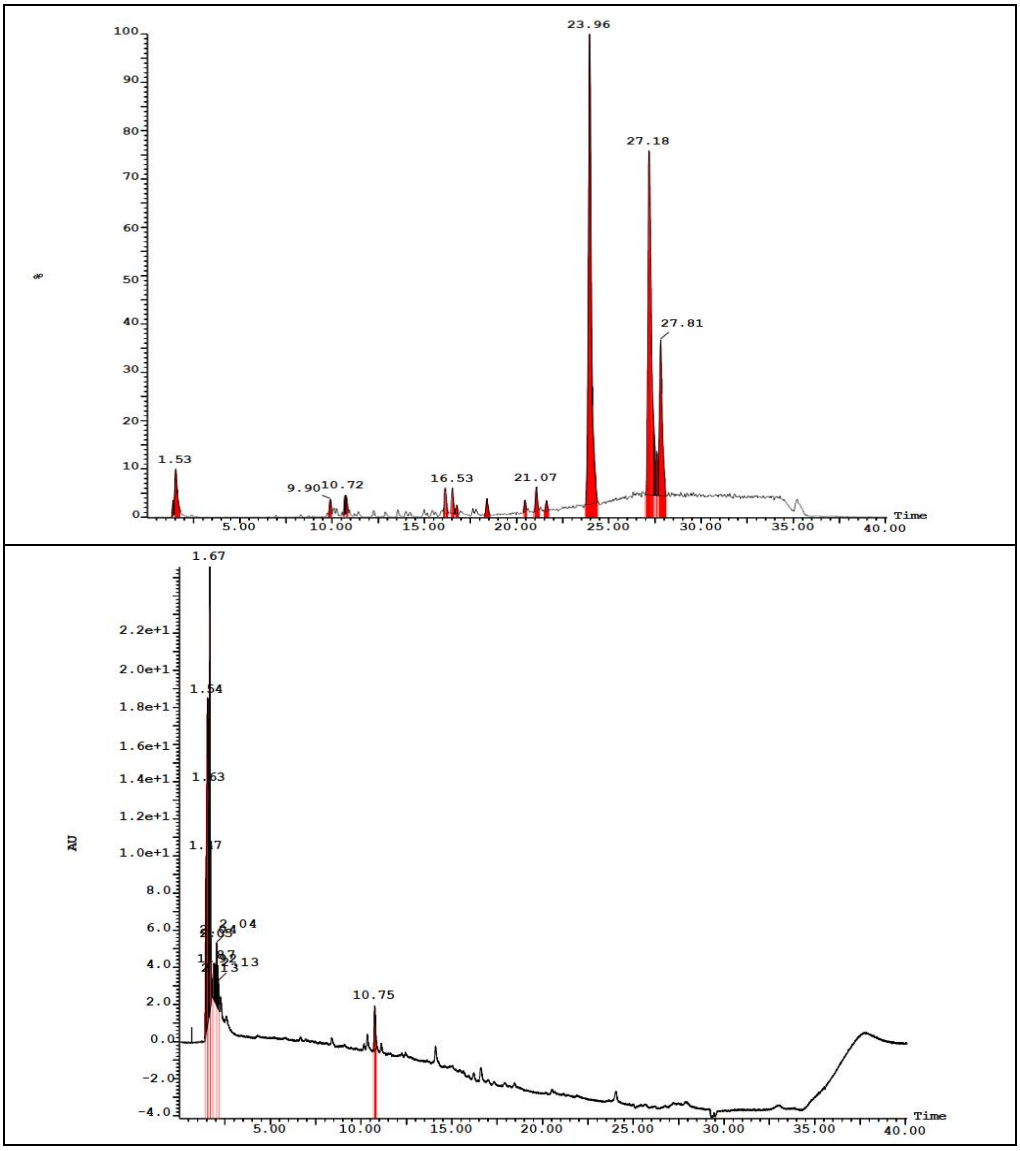

Figure 6: The LC-HRMS Analysis Graph

Table 1: LC–MS-based tentative identification of phytoconstituents with corresponding retention times (RT), observed m/z values, suggested compounds, and supporting fragmentation rationale.

Sr. No.	Peak RT (min)	Observed m/z	Suggested Compound	Rationale
1	1.49	325.1	Epigallocatechin	Early RT, fragments 145/163
2	1.75	325.1	Gallocatechin	Isomeric match
3	10.08	284.1	Biochanin A	Exact m/z and fragmentation
4	10.27	314.1	Formononetin	Strong base peak
5	10.68	314.1	Calycosin	Methoxylated isoflavone
6	11.04	314.1	Prunetin	Isomeric compound
7	12.21	346.2	Daidzin	Sugar loss pattern
8	12.62	346.2	Genistin	Glycosidic fragmentation
9	13.56	593.4	Rutin	Disaccharide fragmentation
10	14.92	431.3	Quercetin-3-O-glucoside	Loss of hexose
11	16.52	445.2	Kaempferol-3-O-rhamnoside	Dominant peak
12	17.23	332.2	Medicarpin	Fabaceae marker
13	17.86	302.2	Daidzein	Aglycone
14	17.91	302.2	Genistein	Isomeric confirmation
15	~10–12	195.1	Ferulic acid	Characteristic fragment
16	~10–12	179.1	Caffeic acid	Common plant phenolic

Molecular Docking

The molecular docking study evaluated the interaction of all identified phytoconstituents with α-glucosidase (PDB ID: 7JTY), using the native ligand as a reference standard (Table 2). The native ligand exhibited a docking score of −6.4 kcal/mol, forming conventional hydrogen bonds with ASP640 and ASP305 (bond lengths 2.28–2.77 Å) along with hydrophobic π–sigma interactions with TRP423. This indicates moderate binding affinity and serves as a baseline for comparison.

Among the tested compounds, rutin demonstrated the highest binding affinity (−8.4 kcal/mol) with multiple strong hydrogen bonds involving ASP564, ASP305, CYS524, TRP525, and TRP523, along with electrostatic (ASP640) and extensive hydrophobic interactions with PHE571 and TRP525. Similarly, daidzin (−8.2 kcal/mol) formed strong hydrogen bonds with PHE571 and HIS698, supported by electrostatic interactions with ASP564 and ASP640, indicating enhanced binding stability. Compounds including daidzein, formononetin, epigallocatechin, and gallocatechin (−8.0 kcal/mol) exhibited consistent hydrogen bonding interactions primarily with ASP305, ASP451, and ASP640, along with hydrophobic π–π interactions with PHE571 and TRP525. Calycosin (−7.9 kcal/mol) showed hydrogen bonding with ASP564, MET565, and ARG624, along with π–π and π–alkyl interactions, enhancing binding affinity. Genistein and prunetin (−7.8 kcal/mol) displayed similar interaction profiles involving ASP305 and hydrophobic residues such as PHE571 and VAL576.

Biochanin A (−7.6 kcal/mol) exhibited hydrogen bonding with ASP305 and ASP640, along with electrostatic and hydrophobic interactions involving PHE571, TRP525, and VAL576. Genistin (−7.5 kcal/mol) showed hydrogen bonding with ASP451 and electrostatic interaction with ASP564, while kaempferol-3-O-rhamnoside (−7.5 kcal/mol) formed strong hydrogen bonds with ASP305 and ARG624. Medicarpin (−7.5 kcal/mol) also demonstrated stable binding through hydrogen bonding with ASP564 and ARG624, along with hydrophobic interactions. Quercetin-3-O-glucoside (−7.2 kcal/mol) formed multiple hydrogen bonds with ASP305, ASP640, and PHE307, supported by hydrophobic interactions with PHE571 and TRP525. Caffeic acid (−6.7 kcal/mol) showed hydrogen bonding with ASP451, ASP305, and ARG624, along with electrostatic and hydrophobic interactions, whereas ferulic acid (−6.5 kcal/mol) exhibited hydrogen bonding with ASP451 and HIS698.

Overall, most phytoconstituents demonstrated stronger binding affinity than the native ligand. Key active site residues such as ASP305, ASP640, ASP564, ASP451, TRP525, and PHE571 were consistently involved in ligand binding through hydrogen bonding, electrostatic, and hydrophobic interactions. The presence of multiple interaction types and shorter bond lengths contributed to enhanced stability of ligand–protein complexes. These findings suggest that compounds such as rutin, daidzin, daidzein, epigallocatechin, and calycosin possess significant inhibitory potential against α-glucosidase and may serve as promising candidates for the management of T2DM. The 2D and 3D binding interaction poses of most potent compounds with alpha glucosidase are shown in Table 3.

Table 2: Binding interactions of selected compounds with alpha glucosidase

Amino Acid	**Bond Length**	**Bond Type**	**Bond Category**	**Ligand Energy**	**Docking Score**
				(Kcal/mol)	
Native Ligand					
ASP640	2.48649	Hydrogen Bond	Conventional Hydrogen Bond	1455.85	-6.4
ASP305	2.2827				
ASP305	2.77419				
TRP423	3.99185	Hydrophobic	Pi-Sigma		
TRP423	3.60887				
Biochanin_A					
ASP305	3.36234	Hydrogen Bond	Carbon Hydrogen Bond	194.96	-7.6
ASP640	3.63331				
ASP305	4.27313	Electrostatic	Pi-Anion		
ASP640	3.79123				
MET565	4.97393	Other	Pi-Sulfur		
PHE571	5.09762	Hydrophobic	Pi-Pi Stacked		
PHE571	4.80915				
PHE307	5.34911		Pi-Pi T-shaped		
TRP525	4.81186				

VAL576	5.40374		Pi-Alkyl		
VAL576	4.58362				
Caffeic_acid					
ASP451	1.97908	Hydrogen Bond	Conventional Hydrogen Bond	59.2	-6.7
ASP305	2.30091				
ARG624	2.4585				
ASP640	3.45176	Electrostatic	Pi-Anion		
MET565	5.26285	Other	Pi-Sulfur		
TRP525	5.04636	Hydrophobic	Pi-Pi T-shaped		
Calycosin					
ASP564	2.40273	Hydrogen Bond	Conventional Hydrogen Bond	198.56	-7.9
MET565	3.04229				
ARG624	2.50814				
ASP305	3.91155	Electrostatic	Pi-Anion		
ASP640	3.49516				
TRP423	3.83741	Hydrophobic	Pi-Sigma		
PHE571	4.87441		Pi-Pi Stacked		
PHE571	5.50322				
PHE307	5.1554		Pi-Pi T-shaped		
TRP525	4.81715				
VAL576	4.7215		Pi-Alkyl		
Daidzein					
ASP305	3.67118	Hydrogen Bond	Carbon Hydrogen Bond	171.13	-8
MET565	5.13086	Other	Pi-Sulfur		
PHE571	4.14472	Hydrophobic	Pi-Pi Stacked		
PHE571	4.00412				
TRP525	4.77973		Pi-Pi T-shaped		
VAL576	5.41365		Pi-Alkyl		
VAL576	5.41652				
Daidzin					
PHE571	1.88001	Hydrogen Bond	Conventional Hydrogen Bond	321.11	-8.2
HIS698	2.02134				
ASP564	3.96862	Electrostatic	Pi-Anion		
ASP640	3.87341				
PHE307	4.85117	Hydrophobic	Pi-Pi Stacked		
TRP525	4.7277		Pi-Pi T-shaped		
Epigallocatechin					
ASP451	2.18655	Hydrogen Bond	Conventional Hydrogen Bond	261.1	-8
HIS698	2.79685				
ASP640	1.80431				
ASP564	4.15114	Electrostatic	Pi-Anion		
TRP525	3.80933	Hydrophobic	Pi-Sigma		
PHE307	4.74982		Pi-Pi Stacked		
TRP423	4.67312				
PHE673	4.68112				
TRP423	5.48447				
Ferulic acid					

ASP451	1.90671	Hydrogen Bond	Conventional Hydrogen Bond	85.35	-6.5
HIS698	2.78993				
HIS700	3.67578		Carbon Hydrogen Bond		
ASP640	3.71385	Electrostatic	Pi-Anion		
TRP525	4.82414	Hydrophobic	Pi-Pi T-shaped		
Formononetin					
ASP305	3.66843	Hydrogen Bond	Carbon Hydrogen Bond	171.13	-8
MET565	5.12101	Other	Pi-Sulfur		
PHE571	4.15053	Hydrophobic	Pi-Pi Stacked		
PHE571	4.01011				
TRP525	4.77499		Pi-Pi T-shaped		
VAL576	5.41161		Pi-Alkyl		
VAL576	5.4104				
Gallocatechin					
ASP640	2.4529	Hydrogen Bond	Conventional Hydrogen Bond	259.42	-8
ASP564	4.14457	Electrostatic	Pi-Anion		
TRP525	3.80118	Hydrophobic	Pi-Sigma		
PHE307	4.76668		Pi-Pi Stacked		
TRP423	4.68224				
PHE673	4.68186				
TRP423	5.49278				
Genistein					
ASP305	3.69233	Hydrogen Bond	Carbon Hydrogen Bond	181.94	-7.8
MET565	5.11889	Other	Pi-Sulfur		
PHE571	4.12781	Hydrophobic	Pi-Pi Stacked		
PHE571	4.01167				
TRP525	4.76392		Pi-Pi T-shaped		
VAL576	5.42449		Pi-Alkyl		
VAL576	5.41922				
Genistin					
ASP451	2.76051	Hydrogen Bond	Conventional Hydrogen Bond	925.29	-7.5
ASP451	2.07387				
ASP564	3.86381	Electrostatic	Pi-Anion		
VAL576	3.74628	Hydrophobic	Pi-Sigma		
VAL576	3.80262				
TRP525	4.7688		Pi-Pi T-shaped		
Kaempferol-3-O-rhamnoside					
ASP305	2.2742	Hydrogen Bond	Conventional Hydrogen Bond	290.61	-7.5
ARG624	1.80246				
ASP640	3.29997	Electrostatic	Pi-Anion		
TRP525	4.61648	Hydrophobic	Pi-Pi T-shaped		
TRP525	5.00185				
HIS700	4.72228				
PHE571	4.27032		Pi-Alkyl		
Medicarpin					
ASP564	2.06065	Hydrogen Bond	Conventional Hydrogen Bond	431.87	-7.5

ARG624	2.03311				
ASP305	3.34369		Carbon Hydrogen Bond		
ASP305	3.31223				
ASP640	3.6731	Electrostatic	Pi-Anion		
PHE307	3.85283	Hydrophobic	Pi-Sigma		
TRP525	5.20596		Pi-Pi T-shaped		
PHE673	5.05343				
TRP525	4.82623		Pi-Alkyl		
Prunetin					
ASP451	2.46988	Hydrogen Bond	Conventional Hydrogen Bond	195.5	-7.8
ASP564	4.00754	Electrostatic	Pi-Anion		
ASP640	4.01796				
PHE307	4.96284	Hydrophobic	Pi-Pi Stacked		
TRP525	4.66419		Pi-Pi T-shaped		
TRP525	5.80938				
Quercetin-3-O-glucoside					
ASP305	2.5279	Hydrogen Bond	Conventional Hydrogen Bond	825.04	-7.2
ASP305	2.33615				
ASP640	2.50422				
PHE307	2.05853				
VAL306	3.44766		Carbon Hydrogen Bond		
PHE571	3.89688	Hydrophobic	Pi-Pi Stacked		
PHE571	4.5428				
PHE307	4.86023		Pi-Pi T-shaped		
TRP525	5.24285				
VAL576	4.50572		Pi-Alkyl		
Rutin					
ASP564	3.08006	Hydrogen Bond	Conventional Hydrogen Bond	1617.7	-8.4
ASP305	2.7371				
CYS524	2.51609				
TRP525	2.00535				
TRP523	2.35847				
ASP640	3.37007	Electrostatic	Pi-Anion		
PHE571	4.27984	Hydrophobic	Pi-Pi Stacked		
PHE307	5.69567				
TRP525	4.68852		Pi-Pi T-shaped		
TRP525	4.93976				
TRP525	5.07574				
HIS700	4.65569				
TRP525	4.8483		Pi-Alkyl		

Table 3: 2D and 3D binding interaction poses of most potent compound with alpha glucosidase

3D Binding Interaction	**2D Binding Interaction**
Native Ligand	
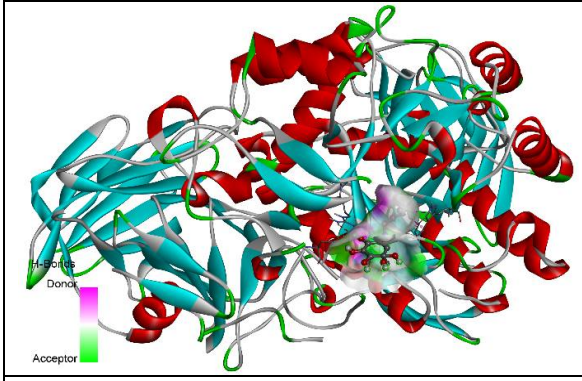	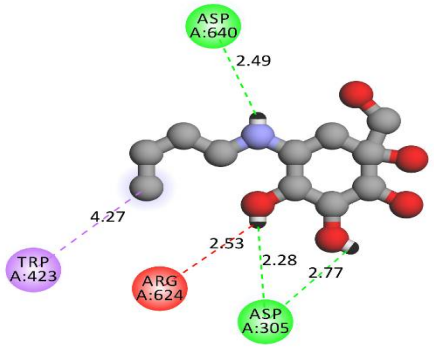
Biochanin A	

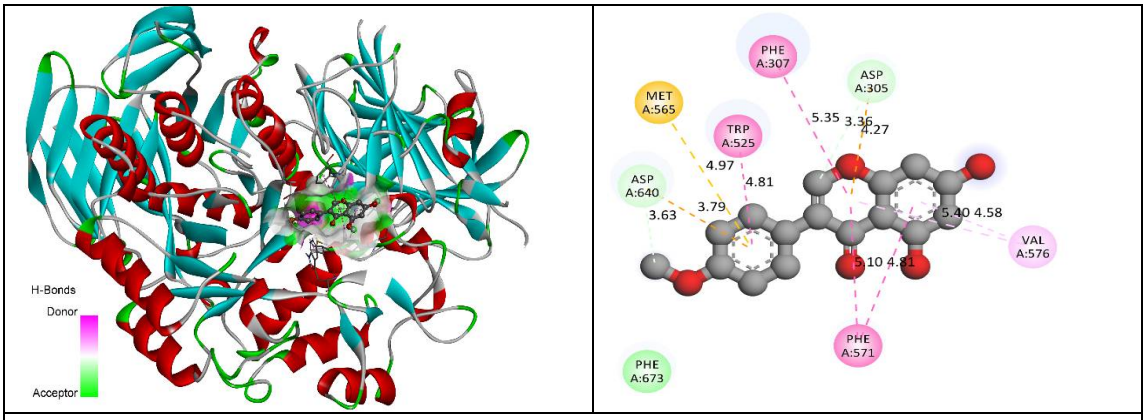

Caffeic acid

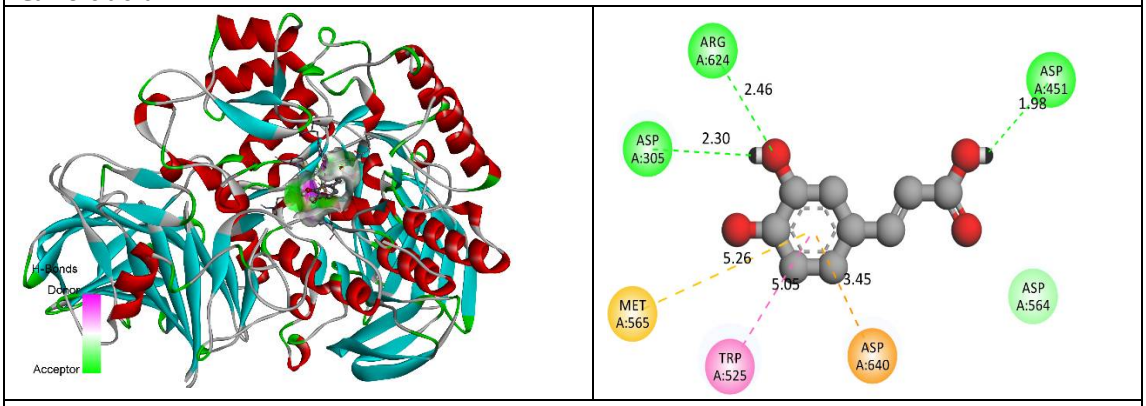

Calycosin

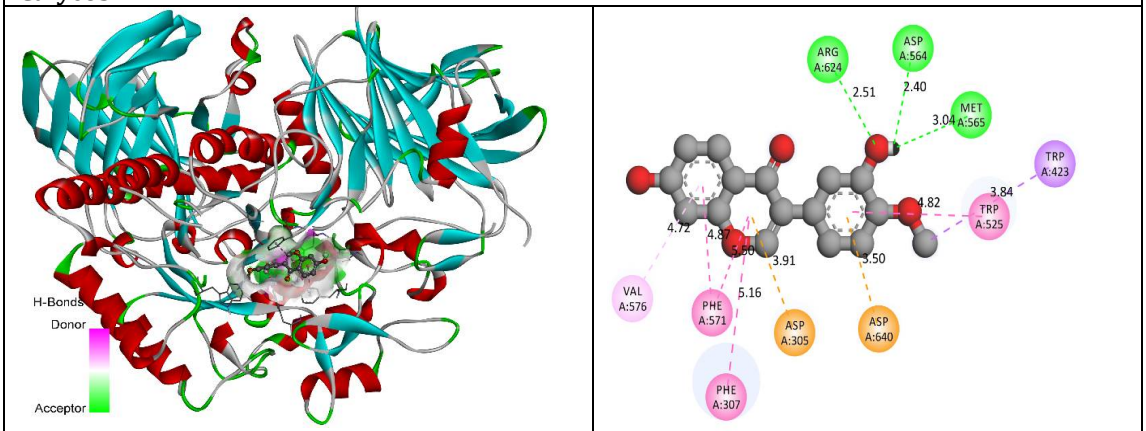

Daidzein

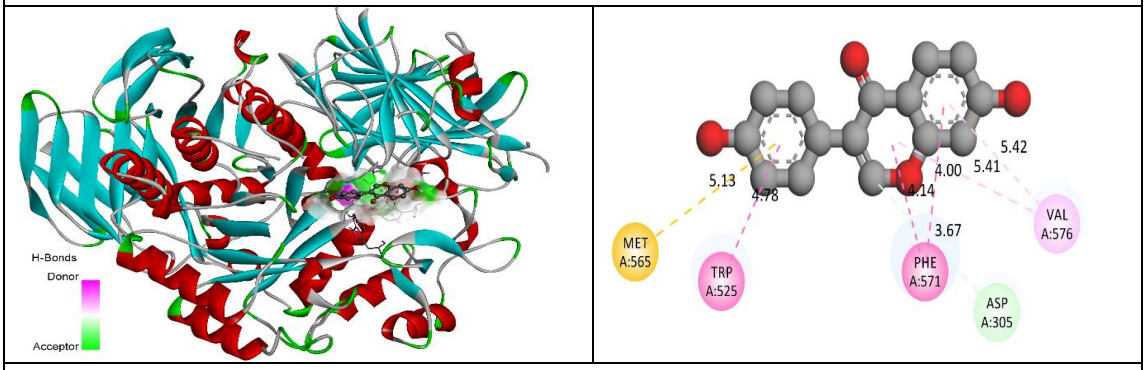

Daidzin

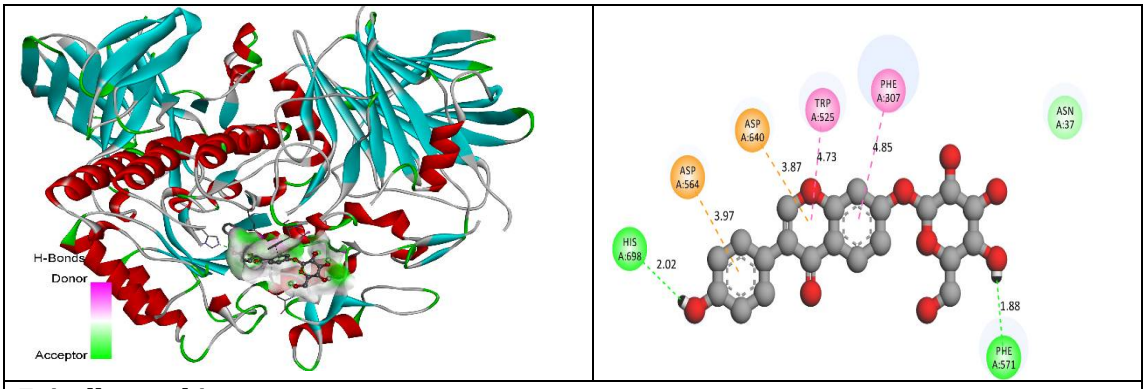

Epigallocatechin

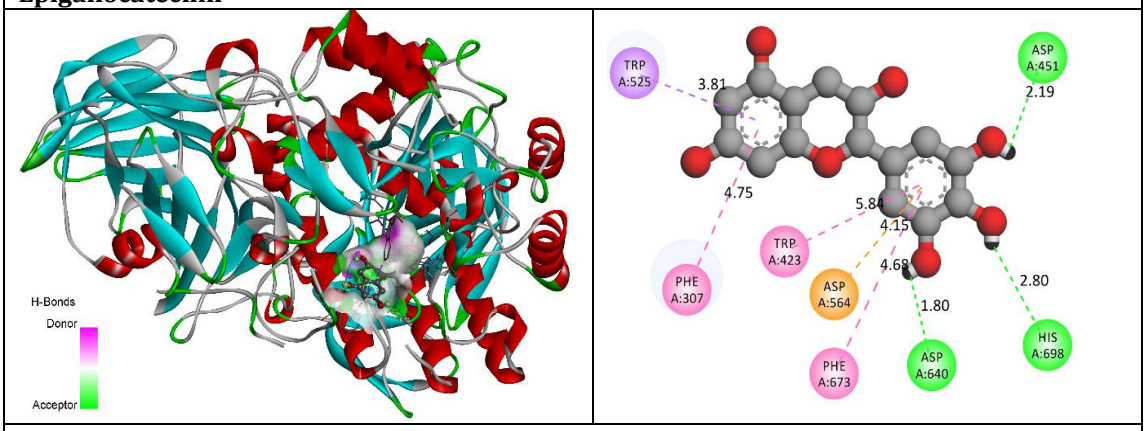

Ferulic acid

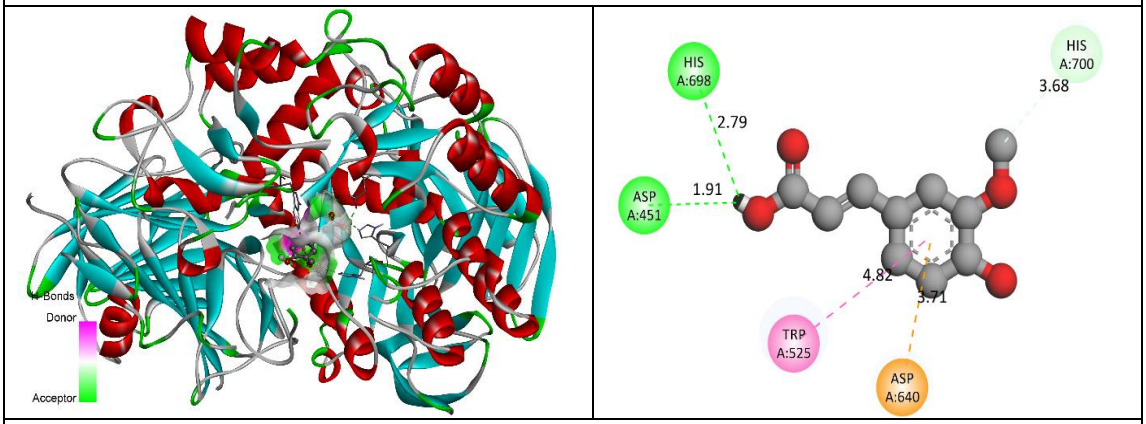

Formononetin

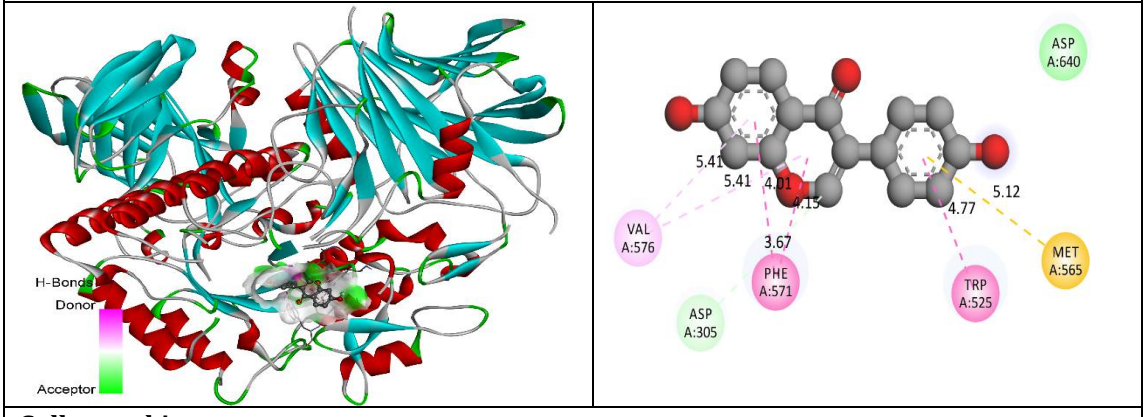

Gallocatechin

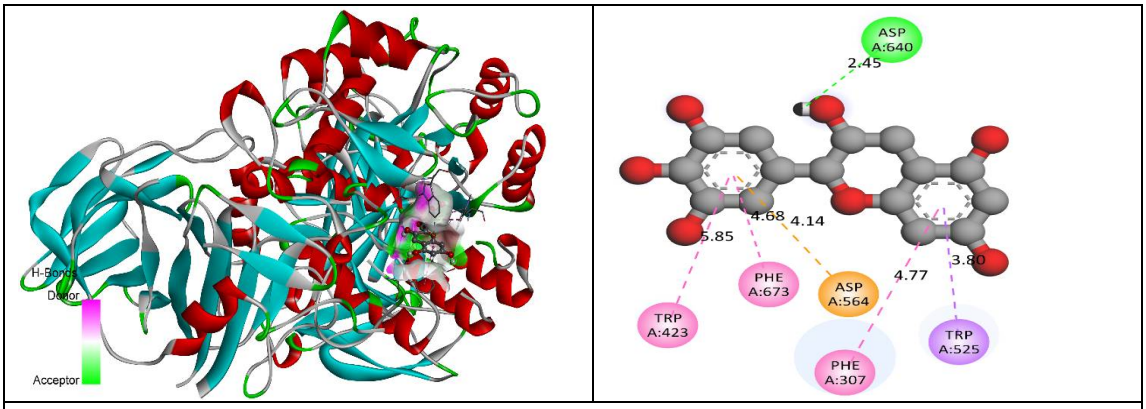

Genistein

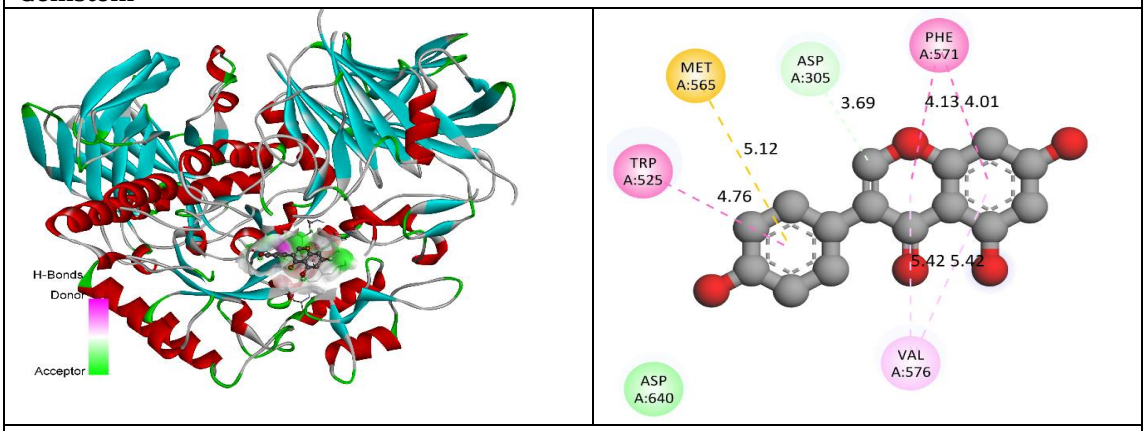

Genistin

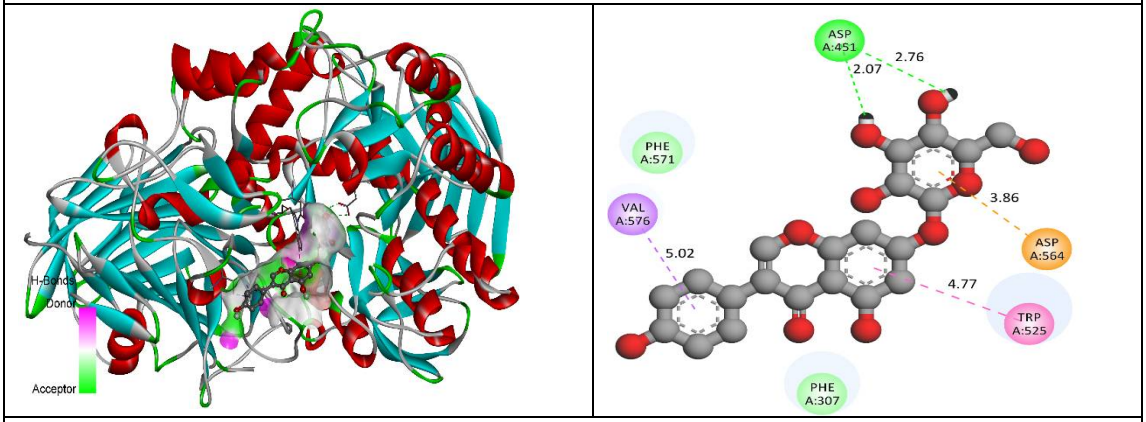

Kaempferol-3-O-rhamnoside

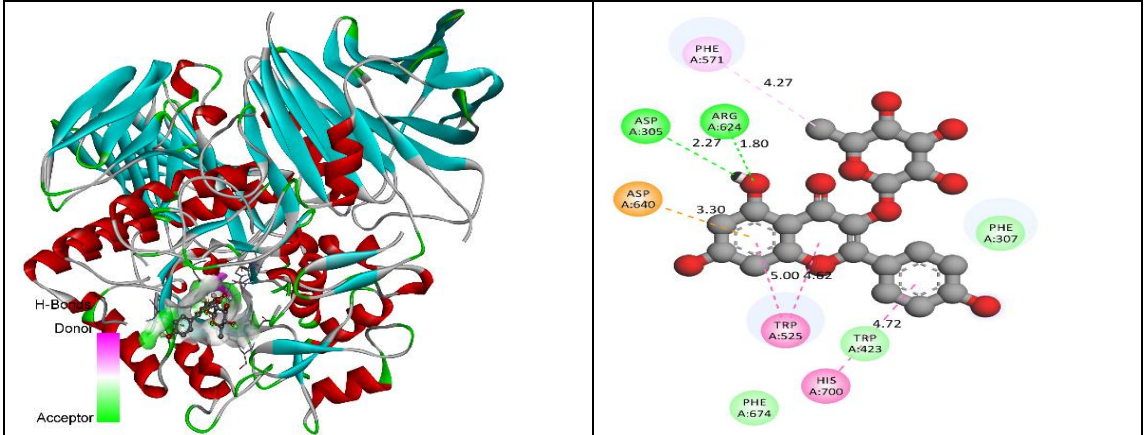

Medicarpin

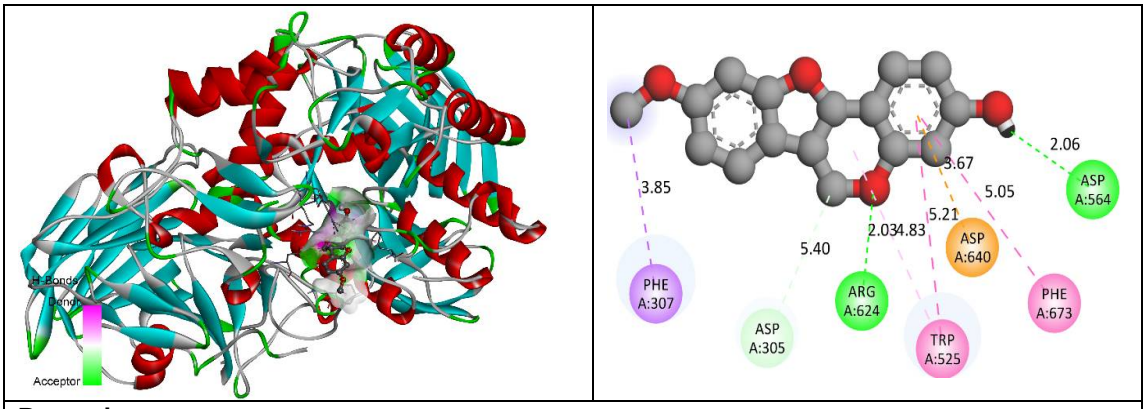

Prunetin

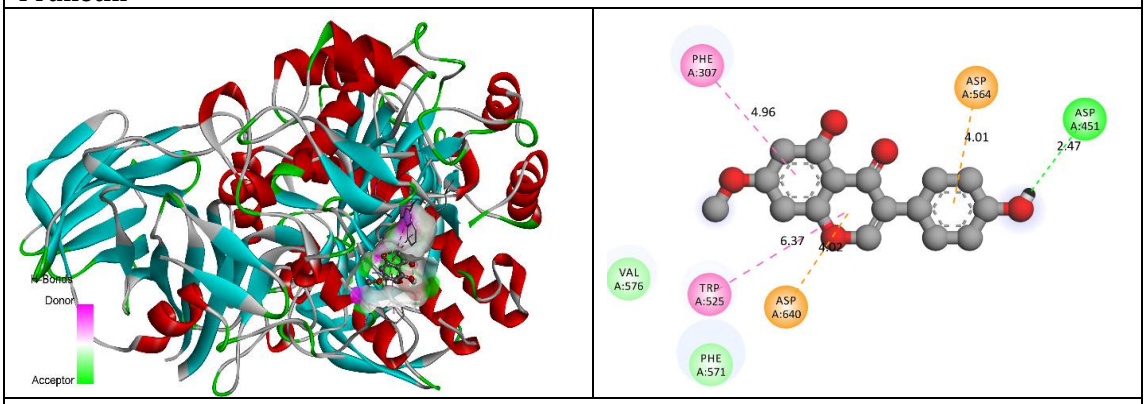

Quercetin-3-O-glucoside

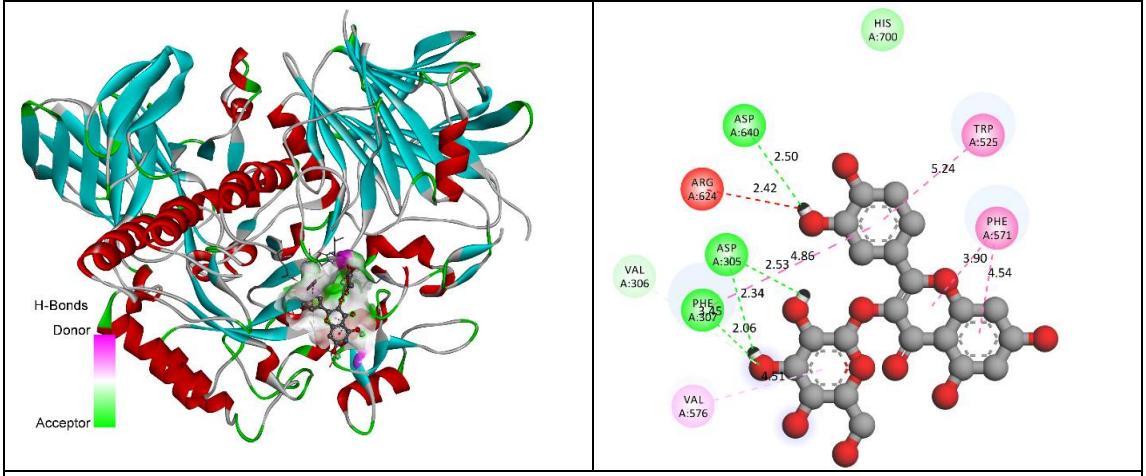

Rutin

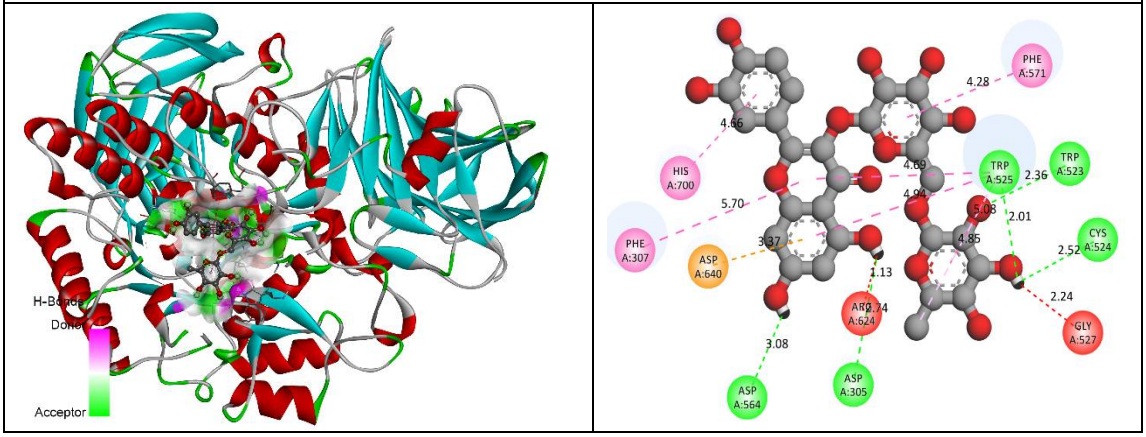

ADMET Analysis

Physicochemical Properties

The physicochemical characteristics of the selected compounds revealed considerable structural diversity, with molecular weights ranging from 180.04 to 610.15. The native ligand exhibited moderate molecular weight (249.16), higher polarity (TPSA 113.18 $Å^2$), and low lipophilicity (logP −0.22), indicating good solubility but relatively limited membrane permeability. In contrast, aglycone flavonoids such as biochanin A, genistein, and medicarpin demonstrated optimal lipophilicity (logP ∼2–3), which favors passive diffusion across biological membranes. Glycosylated derivatives, including rutin and quercetin-3-O-glucoside, showed elevated TPSA values (>200 $Å^2$), suggesting reduced permeability. Hydrogen bonding parameters were within acceptable limits for most compounds except glycosides. Overall, several phytoconstituents displayed improved balance between solubility and permeability compared to native ligand. Physicochemical properties of the native ligand and selected phytoconstituents identified from the ethyl acetate fraction of *Rhynchosia rothii* are shown in Table 4.

Table 4: Physicochemical properties of the native ligand and selected phytoconstituents identified from the ethyl acetate fraction of *Rhynchosia rothii.*

Compounds	MW	Volume	Dense	nHA	nHD	nRot	nRing	TPSA	logS	logP
Native Ligand	249.16	245.2037	1.016135	6	6	5	1	113.18	-0.6624	-0.22732
Biochanin A	284.07	282.4823	1.00562	5	2	2	3	79.9	-3.72479	2.410735
Caffeic acid	180.04	177.6425	1.013496	4	3	2	1	77.76	-1.83711	1.189631
Calycosin	284.07	282.4823	1.00562	5	2	2	3	79.9	-3.50025	1.784293
Daidzein	254.06	256.3961	0.990889	4	2	1	3	70.67	-3.78991	2.220685
Daidzin	416.11	395.5667	1.051934	9	5	4	4	149.82	-3.38222	0.629997
Epigallocatechin	306.07	288.0397	1.062597	7	6	1	3	130.61	-2.50674	0.793661
Ferulic acid	194.06	194.9385	0.995494	4	2	3	1	66.76	-2.36392	1.647679
Formononetin	254.06	256.3961	0.990889	4	2	1	3	70.67	-3.78991	2.220685
Gallocatechin	306.07	288.0397	1.062597	7	6	1	3	130.61	-2.18763	0.430093
Genistein	270.05	265.1863	1.018341	5	3	1	3	90.9	-3.47115	2.074759
Genistin	432.11	404.3569	1.068635	10	6	4	4	170.05	-3.42984	0.791665
Kaempferol-3-O-rhamnoside	432.11	404.3569	1.068635	10	6	3	4	170.05	-3.94433	1.275369
Medicarpin	270.09	270.4085	0.998822	4	1	1	4	47.92	-4.24054	3.040553
Prunetin	284.07	282.4823	1.00562	5	2	2	3	79.9	-3.30079	2.270298
Quercetin-3-O-glucoside	464.1	421.9374	1.099926	12	8	4	4	210.51	-3.74967	0.632622
Rutin	610.15	552.3177	1.104708	16	10	6	5	269.43	-2.39666	0.986122

Drug-Likeness Evaluation

The drug-likeness assessment indicated variability among the compounds, with the native ligand showing a relatively low QED value (0.313), reflecting moderate drug-likeness (Table 5). In comparison, compounds such as medicarpin (0.865), biochanin A, calycosin, and prunetin (∼0.75) exhibited significantly higher QED values, suggesting superior drug-like characteristics. Most compounds complied with Lipinski's rule of five, indicating good oral bioavailability potential. However, glycosylated compounds like rutin and quercetin-3-O-glucoside showed rule violations due to high molecular weight and polarity. The natural product scores were notably high for epigallocatechin and gallocatechin (>2), indicating structural complexity and biological relevance. Overall, several phytoconstituents demonstrated enhanced drug-likeness compared to the native ligand, supporting their suitability as lead molecules.

Table 5: Drug-likeness evaluation of the native ligand and selected compounds based on QED, natural product score, and rule-based filters.

Compounds	QED	NP Score	Lipinski rule	Pfizer Rule	GSK Rule	Golden Triangle	Chelator Rule
Native Ligand	0.313	1.684	0	0	0	0	0
Biochanin A	0.756	1.12	0	0	0	0	0
Caffeic acid	0.472	1.124	0	0	0	1	1
Calycosin	0.756	1.008	0	0	0	0	1
Daidzein	0.7	0.83	0	0	0	0	0
Daidzin	0.406	1.539	0	0	1	0	0
Epigallocatechin	0.437	2.272	0	0	0	0	1
Ferulic acid	0.715	0.926	0	0	0	1	1
Formononetin	0.7	0.83	0	0	0	0	0
Gallocatechin	0.437	2.272	0	0	0	0	1
Genistein	0.632	1.355	0	0	0	0	0
Genistin	0.331	1.932	0	0	1	0	0
Kaempferol-3-O-rhamnoside	0.348	2.075	0	0	1	0	0
Medicarpin	0.865	1.859	0	1	0	0	0
Prunetin	0.756	1.141	0	0	0	0	0
Quercetin-3-O-glucoside	0.229	2.16	1	0	1	0	1
Rutin	0.14	2.015	1	0	1	1	1

Absorption Profile

The absorption profile demonstrated that the native ligand possesses moderate permeability (Caco-2: −5.68) and relatively low human intestinal absorption (HIA ∼0.28), indicating limited oral absorption efficiency. In contrast, smaller phenolic compounds such as caffeic acid and ferulic acid exhibited higher HIA values, suggesting better intestinal uptake. Aglycone flavonoids including biochanin A, daidzein, and formononetin showed improved permeability due to favorable lipophilicity and lower polarity. Glycosylated compounds such as rutin and genistin exhibited poor permeability but moderate absorption, likely mediated by transporter systems. native ligand also showed high probability of being a P-gp substrate, indicating potential efflux and reduced bioavailability. Overall, several phytoconstituents demonstrated better absorption characteristics than the native ligand. Predicted absorption parameters of the native ligand and selected are shown in Table 6.

Table 6: Predicted absorption parameters of the native ligand and selected phytoconstituents, including permeability, P-gp interaction, and intestinal absorption indices**.**

Compounds	Caco-2 Permeability	MDCK Permeability	Pgp-inhibitor	Pgp-substrate	HIA	F20%	F30%	F50%
Native Ligand	-5.68253	-4.93218	1.29E-05	0.997768	0.285195	0.094643	0.824286	0.961573
Biochanin A	-5.00934	-4.82906	0.153813	0.320613	0.085162	0.463976	0.834799	0.962173
Caffeic acid	-4.94034	-4.80109	0.000135	0.011763	0.301189	0.997053	0.995638	0.997994
Calycosin	-4.88636	-4.80434	0.046292	0.303755	0.064601	0.599869	0.854024	0.988162
Daidzein	-4.69247	-4.77484	0.01548	0.36456	0.016927	0.747902	0.848493	0.981537
Daidzin	-6.38035	-5.08407	0.000136	0.104014	0.644242	0.22607	0.947571	0.919048
Epigallocatechin	-6.65989	-4.96038	1.75E-05	0.049045	0.025356	0.983639	0.997253	0.999448
Ferulic acid	-4.98863	-4.79135	0.00451	0.050445	0.249424	0.956667	0.932978	0.993275
Formononetin	-4.69247	-4.77484	0.01548	0.36456	0.016927	0.747902	0.848493	0.981537
Gallocatechin	-6.45054	-4.95012	0.00034	0.08767	0.010368	0.867486	0.98341	0.996059
Genistein	-5.05057	-4.8308	0.005231	0.462178	0.008095	0.520912	0.816296	0.976917
Genistin	-6.41398	-5.06502	7.47E-05	0.412325	0.602662	0.268623	0.976293	0.985196
Kaempferol-3-O-rhamnoside	-6.24466	-5.08446	0.001041	0.756053	0.000128	0.010323	0.072948	0.983832
Medicarpin	-4.78541	-4.7433	0.046958	0.596758	0.000965	0.47064	0.76185	0.935271
Prunetin	-4.83237	-4.78696	0.136672	0.137784	0.031387	0.192095	0.33751	0.911063
Quercetin-3-O-glucoside	-6.36229	-4.95514	5.24E-06	0.097432	0.189164	0.36004	0.998317	0.9998
Rutin	-6.54652	-5.02701	6.22E-08	0.699256	0.639735	0.772111	0.999751	0.999936

Distribution and Metabolism

The distribution and metabolic profiles of native ligand and phytoconstituents showed notable differences (Table 7). Native ligand exhibited low plasma protein binding (42.18%) and a high free fraction (60.27%), indicating better bioavailability and wider tissue distribution. In contrast, most phytoconstituents, including biochanin A, genistein, and prunetin, showed high protein binding (>80%), suggesting prolonged circulation but reduced free drug availability. BBB permeability was minimal for most compounds, except medicarpin, which showed relatively higher permeability, indicating potential CNS access.

Metabolically, Native ligand displayed negligible interaction with CYP450 enzymes, suggesting low risk of drug–drug interactions. Conversely, aglycone compounds such as biochanin A, genistein, daidzein, and prunetin exhibited strong interactions with CYP1A2, CYP2C9, and CYP3A4 (Table 7), indicating higher metabolic susceptibility. Glycosylated derivatives demonstrated weaker interactions due to increased polarity. Overall, native ligand showed favorable pharmacokinetics, whereas phytoconstituents exhibited variable metabolic behavior.

Table 7: Distribution and metabolism profiles of the native ligand and selected compounds, including plasma protein binding, BBB permeability, and CYP450 interactions.

Compounds	Distribution				Metabolism									
					CYP1A2		CYP2C19		CYP2C9		CYP2D6		CYP3A4	
	PPB%	VD	BBB	Fu	Inhibitor	Substrate	Inhibitor	Substrate	Inhibitor	Substrate	Inhibitor	Substrate	Inhibitor	Substrate
Native Ligand	42.18615	-0.09225	0.136884	60.27218	0.007518	0.003149	6.27E-05	1.97E-06	0.002658	0.015247	0.136171	0.000857	7.07E-05	6.56E-05
Biochanin A	97.16405	-0.0814	0.015025	2.087907	0.99822	0.999791	0.94741	0.000154	0.294531	0.987464	0.99756	0.999947	0.989567	7.77E-06
Caffeic acid	64.66704	-0.60576	0.001788	32.16007	0.005847	4.99E-05	1.89E-05	0.000835	0.004228	0.031208	0.000198	0.002296	0.001152	2.60E-05
Calycosin	91.18846	-0.53686	0.008946	7.949163	0.998675	0.976413	0.98837	0.005287	0.760217	0.989487	0.982522	0.988595	0.132466	0.000554
Daidzein	91.8024	-0.20983	0.024719	11.86281	0.994319	0.99754	0.998658	0.002312	0.996348	0.984585	0.999615	0.999961	0.856628	1.32E-05
Daidzin	78.49698	-0.13796	0.007096	22.1191	0.000223	0.112341	0.006203	1.80E-05	0.033681	0.066417	0.030193	0.138502	0.000458	1.35E-07

0.515399	0.000224	1.32E-05	0.070916	4.09E-05	3.06E-07	8.70E-06	0.823809	3.34E-06	2.87E-07	2.29E-09
0.003498	0.00035	0.856628	0.017287	0.991745	0.000875	0.583995	0.857556	0.937377	0.805414	0.029205
1.38E-06	0.016114	0.999961	0.000999	0.999877	0.014299	0.010412	0.999756	0.999852	0.0192	1.48E-07
1.80E-09	0.001132	0.999615	6.38E-08	0.99681	0.002658	0.000501	0.927042	0.984878	2.73E-06	2.26E-06
0.000234	0.13468	0.984585	0.00772	0.86663	0.006639	0.029869	0.963935	0.997365	0.001345	7.47E-05
0.001232	0.018414	0.996348	0.001908	0.308506	0.000169	0.002706	0.796981	0.261337	5.70E-05	1.85E-06
4.40E-06	0.016178	0.002312	0.002239	0.000216	4.85E-07	3.69E-05	0.938499	0.001676	3.22E-06	1.07E-06
2.69E-07	0.000783	0.998658	7.21E-07	0.859612	8.25E-06	0.003081	0.921586	0.956534	8.27E-08	1.44E-07
0.994658	0.000272	0.99754	0.727946	0.994849	0.068927	0.037651	0.965826	0.990343	0.013423	0.00364
1.64E-05	0.018324	0.994319	1.41E-05	0.999333	0.000101	0.077727	0.992473	0.99985	0.001357	0.0001
19.43889	25.19214	11.86281	15.46776	5.766246	16.73398	9.863648	14.70272	4.903012	15.14114	14.65911
0.036949	0.001125	0.024719	0.019268	0.03145	0.007908	4.22E-06	0.617057	0.035065	0.000205	3.59E-05
0.037232	-0.72683	-0.20983	-0.04336	-0.42588	-0.14797	-0.07643	-0.01678	-0.22738	-0.07266	-0.05883
89.3651	68.60053	91.8024	89.2805	95.86518	82.26085	89.04325	86.2244	94.83271	83.13148	85.0054
Epigallocatechin	Ferulic acid	Formononetin	Gallocatechin	Genistein	Genistin	Kaempferol-3-O-rhamnoside	Medicarpin	Prunetin	Quercetin-3-O-glucoside	Rutin

Excretion and Toxicity

The excretion and toxicity profiles revealed distinct differences among native ligand and phytoconstituents (Table 8). Native ligand showed moderate clearance (3.35) and half-life (~1.96 h), indicating balanced elimination. Several phytoconstituents, such as caffeic acid and epigallocatechin, exhibited higher clearance and slightly prolonged half-life, suggesting sustained activity. Glycosides like rutin and genistin demonstrated lower clearance but longer half-life, indicating extended retention.

Toxicity assessment indicated that native ligand possesses low hepatotoxicity (DILI) and acceptable safety. Phenolic acids, including caffeic acid and ferulic acid, showed favorable safety profiles with low toxicity. However, glycosylated compounds such as rutin and genistin exhibited higher DILI and Ames toxicity probabilities (Table 8), likely due to complex metabolism. Most compounds showed low carcinogenicity and acceptable irritation profiles. Overall, several phytoconstituents demonstrated comparable or improved safety profiles relative to native ligand, with phenolic acids emerging as safer candidates.

Table 8: Excretion and toxicity parameters of the native ligand and selected phytoconstituents, including clearance, half-life, and predicted toxicity endpoints.

Compounds	Excretion		Toxicity								
	CL-plasma	T1/2	H-HT	DILI	Ames Toxicity	Rat Oral Acute Toxicity	FDAMDD	Skin Sensitization	Carcinogenicity	Eye Corrosion	Eye Irritation	Respiratory Toxicity
Native Ligand	3.354748	1.963733	0.694345	0.029084	0.322953	0.082354	0.212124	0.828601	0.167872	0.016851	0.797062	0.156004
Biochanin A	5.44645	0.857733	0.464638	0.897894	0.660879	0.525885	0.780214	0.335642	0.745968	0.059895	0.984707	0.843586
Caffeic acid	14.35792	2.070125	0.682861	0.690357	0.27381	0.079248	0.303146	0.975502	0.17864	0.848323	0.998627	0.459408
Calycosin	3.356036	1.601212	0.476387	0.627937	0.610896	0.533567	0.764073	0.413481	0.772234	0.159145	0.989561	0.798657
Daidzein	7.853864	1.176569	0.474093	0.442961	0.537002	0.568507	0.775145	0.480756	0.744253	0.273828	0.992936	0.695835
Daidzin	3.093921	3.27149	0.735119	0.935468	0.892444	0.064707	0.074026	0.977183	0.42972	2.92E-05	0.406406	0.032424

0.857248	0.607863	0.695835	0.674624	0.766274	0.029435	0.123011	0.681249	0.722324	0.051654	0.030272
0.988247	0.996626	0.992936	0.996349	0.99348	0.345983	0.95499	0.983527	0.976936	0.897102	0.904546
0.014281	0.761168	0.273828	0.014224	0.106084	6.01E-06	0.001456	0.105863	0.068736	0.000198	3.59E-05
0.225772	0.248972	0.744253	0.295792	0.6695	0.318037	0.232543	0.636314	0.712451	0.329572	0.046632
0.999779	0.743	0.480756	0.995355	0.60086	0.983326	0.681718	0.575712	0.356734	0.996454	0.997444
0.868492	0.194257	0.775145	0.844307	0.807027	0.059072	0.426758	0.460195	0.645856	0.199878	0.137174
0.517989	0.081005	0.568507	0.420127	0.571784	0.057393	0.112657	0.291375	0.539317	0.053203	0.044139
0.702249	0.25205	0.537002	0.756905	0.556356	0.880999	0.591258	0.649547	0.546236	0.820034	0.756376
0.692126	0.635605	0.442961	0.338232	0.661655	0.968365	0.568876	0.67428	0.822442	0.847297	0.936922
0.514925	0.701876	0.474093	0.632345	0.46065	0.666578	0.331485	0.584746	0.47684	0.467863	0.406325
2.212532	1.697795	1.176569	2.235709	1.112957	3.37487	2.867809	2.762061	0.897354	3.721857	4.616005
11.63066	8.358844	7.853864	11.27579	6.254917	3.153744	2.911451	5.973719	7.284313	3.535791	1.610724
Epigallocatechin	Ferulic acid	Formononetin	Gallocatechin	Genistein	Genistin	Kaempferol-3-O-rhamnoside	Medicarpin	Prunetin	Quercetin-3-O-glucoside	Rutin

Environmental Toxicity

The environmental toxicity assessment indicated that native ligand has a low bioconcentration factor (BCF 0.22), suggesting minimal ecological accumulation (Table 9). Similar trends were observed for several phenolic compounds, indicating environmentally safe profiles. Flavonoids such as medicarpin and biochanin A showed relatively higher BCF values (>1), indicating moderate accumulation potential. Toxicity parameters (IGC50, LC50FM, LC50DM) suggested that most compounds exhibit low to moderate environmental toxicity, with higher values indicating reduced ecological risk. Phenolic acids demonstrated comparatively lower toxicity, further supporting their safety. Overall, both native ligand and the selected phytoconstituents exhibited acceptable environmental profiles with minimal ecological concern.

The ADMET evaluation highlights that several phytoconstituents, particularly biochanin A, genistein, daidzein, and medicarpin, possess superior pharmacokinetic and drug-likeness properties compared to the native ligand. While native ligand showed moderate performance, many natural compounds demonstrated improved absorption, distribution, and safety, supporting their potential as promising candidates for T2DM management. Comparative ADMET radar analysis of the native ligand and selected phytoconstituents are shown in Table 10.

Table 9: Environmental toxicity profile of the native ligand and selected compounds based on bioconcentration and aquatic toxicity indices

Compounds	BCF	IGC50	LC50FM	LC50DM
Native Ligand	0.223695	2.065201	2.563985	3.388117
Biochanin A	1.268545	4.009506	4.379791	4.786932
Caffeic acid	0.299446	2.768426	3.512312	3.933473
Calycosin	1.053499	3.614942	3.906035	4.325283
Daidzein	1.229515	3.900498	4.13246	4.435796
Daidzin	0.659898	3.337204	3.926702	4.607776
Epigallocatechin	0.625683	3.130303	3.500725	4.12181
Ferulic acid	0.183638	2.756398	3.238442	3.979393
Formononetin	1.229515	3.900498	4.13246	4.435796
Gallocatechin	0.465865	2.935129	3.408466	3.95662
Genistein	1.267259	3.774496	4.050573	4.429993
Genistin	0.465037	3.072939	3.633802	4.413816
Kaempferol-3-O-rhamnoside	0.91725	3.599806	3.995526	4.571959
Medicarpin	1.399862	3.883041	4.587433	5.332927
Prunetin	1.229751	3.862111	4.15467	4.553991
Quercetin-3-O-glucoside	0.551015	3.182243	3.787965	4.46838
Rutin	0.533413	3.180953	3.927314	4.680011

Table 10: Comparative ADMET radar analysis of the native ligand and selected phytoconstituents highlighting pharmacokinetic suitability.

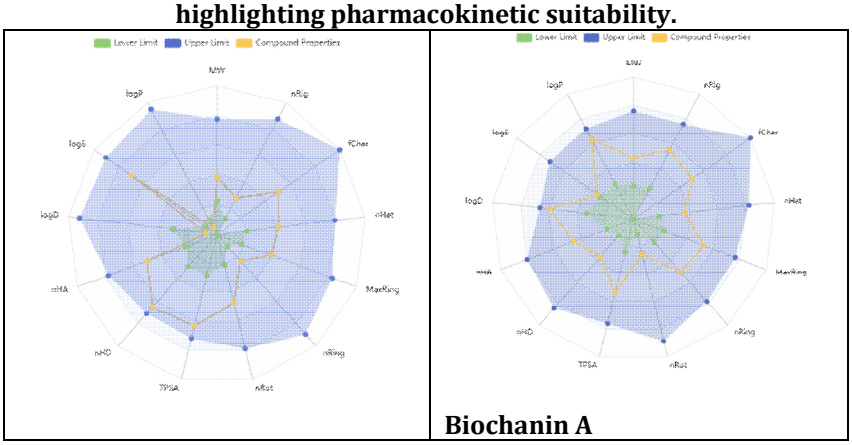

Biochanin A

Native Ligand	
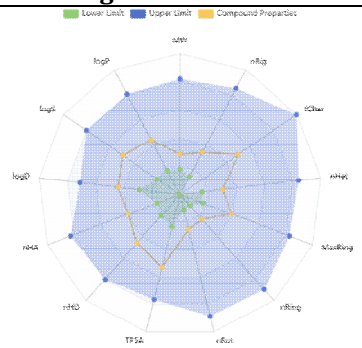 Caffeic acid	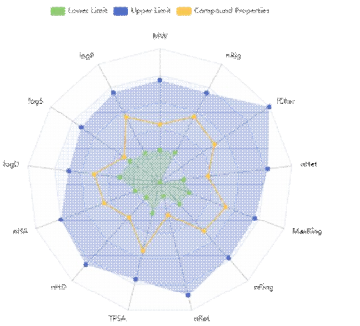 Calycosin
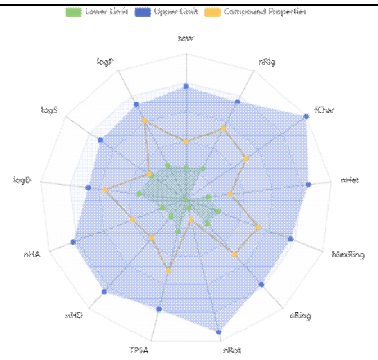 Daidzein	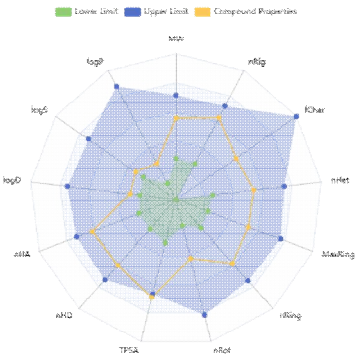 Daidzin
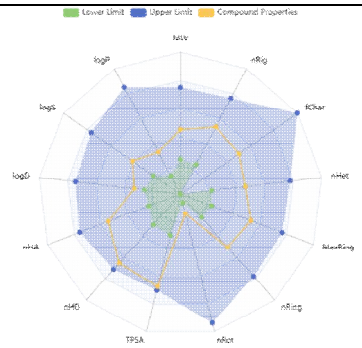 Epigallocatechin	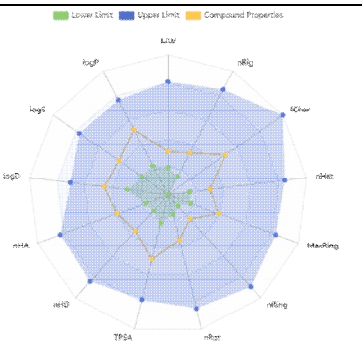 Ferulic acid
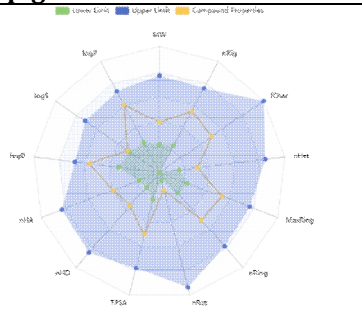 Formononetin	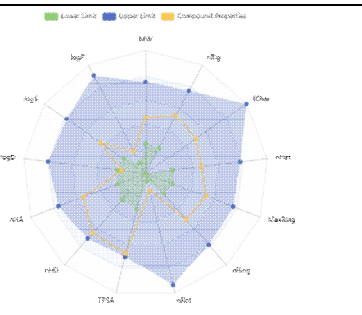 Gallocatechin

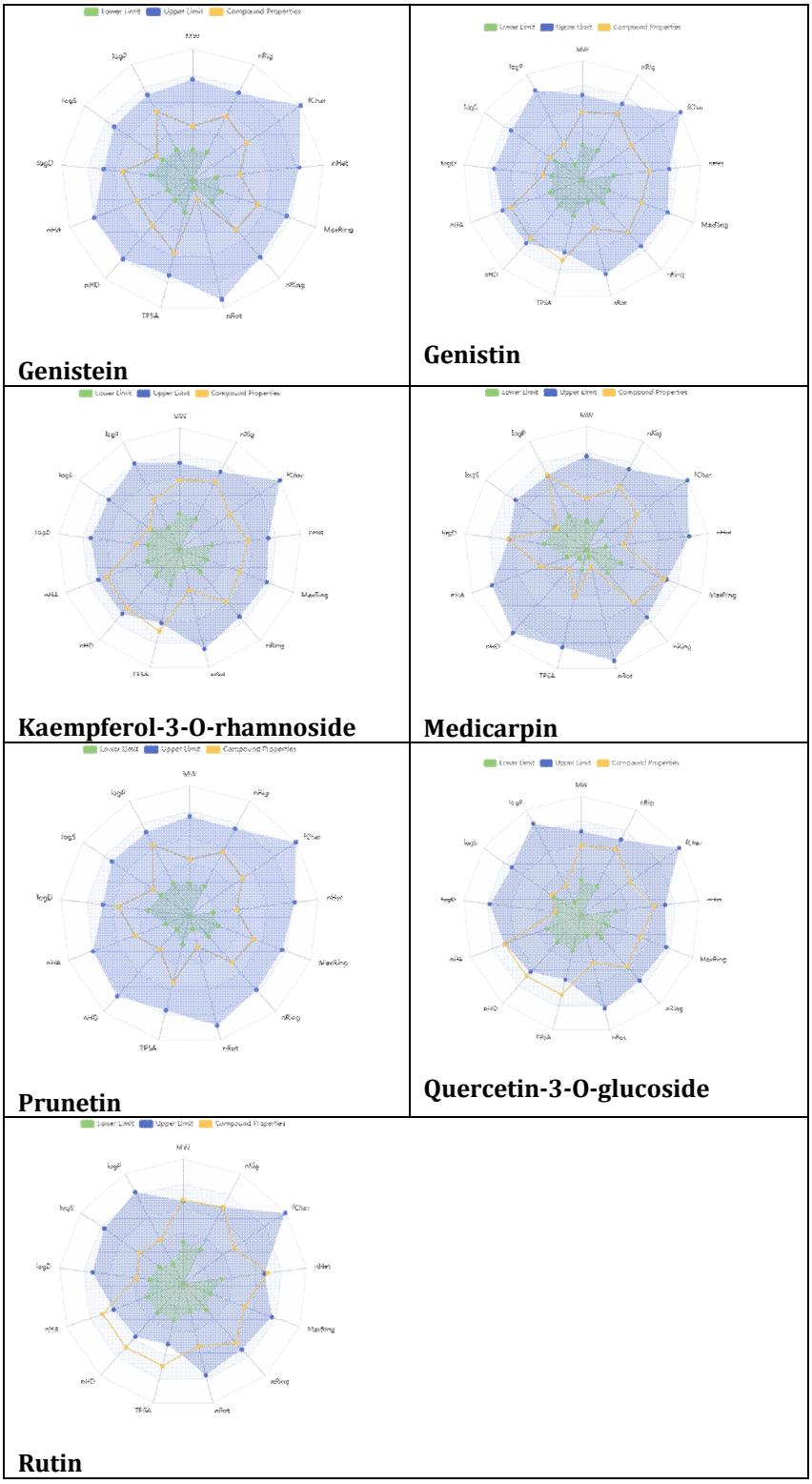

CONCLUSION

The present study comprehensively investigated the phytochemical profile, physicochemical properties, microbial safety, and antidiabetic potential of the ethyl acetate extract of *Rhynchosia rothii*. The extraction process yielded a satisfactory amount of semi-polar constituents, and organoleptic as well as physicochemical evaluations confirmed the quality, purity, and stability of the extract. The absence of microbial contamination further validated its safety for pharmaceutical applications. Qualitative phytochemical screening and LC–HRMS analysis revealed a rich presence of bioactive compounds,

particularly flavonoids, isoflavonoids, and phenolic acids, which are known for their therapeutic potential. Molecular docking studies demonstrated that several compounds, especially rutin, daidzin, daidzein, epigallocatechin, and calycosin, exhibited stronger binding affinity toward α-glucosidase than the native ligand, suggesting promising antidiabetic activity. Furthermore, ADMET analysis indicated that many phytoconstituents possess favorable pharmacokinetic and safety profiles, with improved drug-likeness, absorption, and reduced toxicity compared to the native ligand. Overall, the findings highlight *Rhynchosia rothii* as a potential source of bioactive compounds for the management of type 2 diabetes mellitus. The study supports further in vitro, in vivo, and clinical investigations to validate its therapeutic efficacy and develop novel plant-based antidiabetic agents.

REFERENCES

1. Lamichaney A, Naik SJ S, Hazra KK, Datta D, Parihar AK, Aidbhavi R, Katiyar PK. (2024). Overcoming seed coat–imposed dormancy in wild species of Cajanus and Rhynchosia. Crop Sci., 64, 386–98 https://doi.org /10.1002/csc2.21130.
2. Sharad D. Tayade, Narendra Silawat, Neetesh Jain. (2022). Formulation Development and Evaluation of Herbal Nanoparticles containing Ointment of Leaves extract of Rhynchosia rothii. J. Pharm. Negat. Results, 724–38 https://doi.org/10.47750/pnr.2022.13.s05.113.
3. Tayade SD, Silawat N. (2021). Phytochemical Screening and Wound Healing Activity of Different Leaf Extracts of Rhynchosia rothii in Rats. J. Pharm. Res. Int., 386–93 https://doi.org/10.9734/jpri/2021/v33i46b32953.
4. Tamboli AS, D. Tayade S. (2025). In-Depth Investigation of Berberine and Tropane through Computational Screening as Possible DPP-IV inhibitors for the Treatment of T2DM. J. Pharm. Sci. Comput. Chem., 1, 1–11.
5. Shastri MA, Gadhave R, Talath S, Wali AF, Hani U, Puri S, Rathod B, Khan SL. (2024). In silico Screening, Synthesis, and in vitro Enzyme Assay of Some 1,2,3-Oxadiazole-linked Tetrahydropyrimidine-5-carboxylate Derivatives as DPP-IV Inhibitors for Treatment of T2DM. Chem. Methodol., 8, 800–19 https://doi.org/10.48309 /chemm. 2024.479997.1830.
6. Muralidharan V, Sachdeo RA, Singh LP, Haque MA, Panigrahy UP, Mishra AK, Begum T, Baig MS. (2025). Molecular Docking and Dynamic Simulation with ADMET Exploration of Natural Products Atlas Compound Library to search for Potential Alpha Amylase Inhibitors for the T2DM Treatment. Chem. Methodol., 9, 81–102 https://doi.org/10.48309/chemm.2025.488471.1849.
7. Al-Khayri JM, Sahana GR, Nagella P, Joseph B V., Alessa FM, Al-Mssallem MQ. (2022). Flavonoids as Potential Anti-Inflammatory Molecules: A Review.
8. Balasundram N, Sundram K, Samman S. (2006). Phenolic compounds in plants and agri-industrial by-products: Antioxidant activity, occurrence, and potential uses. Food Chem., 99, 191–203.https://doi.org/ 10.1016/ j.foodchem.2005.07.042.
9. Mizzi L, Chatzitzika C, Gatt R, Valdramidis V. (2020). HPLC analysis of phenolic compounds and flavonoids with overlapping peaks. Food Technol. Biotechnol., 58, 12–9 https://doi.org/10.17113/ftb.58.01.20.6395.
10. Khan SL, Bakshi V. (2026). LC-HRMS and In Silico Analysis of Ailanthus excelsa Metabolites Targeting EGFR Triple Mutation (L858R/T790M/C797S). Adv. J. Chem. Sect. A, 9, 292–311. https://doi.org /10.48309/ ajca.2026.533867.1879.
11. Kızıltaş H, Bingöl Z, Gören AC, Pinar SM, Alwasel SH, Gülçin İ. (2021). LC-HRMS profiling of phytochemicals, antidiabetic, anticholinergic and antioxidant activities of evaporated ethanol extract of *Astragalus brachycalyx* Fischer. J. Chem. Metrol., 15, 135–51 https://doi.org/10.25135/JCM.62.2107.2155.
12. Vasincu A, Luca SV, Charalambous C, Neophytou CM, Skalicka-Woźniak K, Miron A. (2022). LC-HRMS/MS phytochemical profiling of *Vernonia kotschyana* Sch. Bip. ex Walp.: Potential involvement of highly-oxygenated stigmastane-type saponins in cancer cell viability, apoptosis and intracellular ROS production. South African J. Bot., 144, 83–91 https://doi.org/10.1016/j.sajb.2021.09.003.
13. Prathyusha S, Shankar Gupta P, Kumar AK, Hussain Syed S, Shaik M, Jahnavi P, Rani S, Rajashakar V. (2026). Theoretical and Computational Study of Bioactive Compounds from *Myrica nagi* as Inhibitors of Neuroendocrine and Opioid Receptors: A Molecular Docking and Dynamics Approach. Adv. J. Chem. Sect. A, 9, 223–42 https://doi.org/10.48309/ajca.2026.535612.1887.
14. Gheidari D, Mehrdad M, karimelahi Z. (2024). Virtual screening, ADMET prediction, molecular docking, and dynamic simulation studies of natural products as BACE1 inhibitors for the management of Alzheimer's disease. Sci. Rep., 14, 26431 https://doi.org/10.1038/s41598-024-75292-6.
15. Isa AS, Mohammed AM. (2024). Computational Analysis of Novel 4-Thiazolidinone Derivatives as Potential Anti-Breast Cancer Agents: Docking, Pharmacokinetics, and Molecular Dynamics Study&;quot; Med. Med. Chem.
16. Siddiqui Q, Shaikh YA. (2026). Hydroalcoholic Extraction of *Cissus quadrangularis* and In Vitro Evaluation of Antifungal Properties. J. PharmTechNova, 01, 3–10 https://doi.org/10.66220/vyc7rc95.
17. Siddiqui FA, Bakshi V. (2026). GC–MS-based analytical profiling of *Lantana camara* phytoconstituents and computational analysis for multi-target antidiabetic activity. J. Chem. Lett., 7, 1–24 https://doi.org /10.22034/jchemlett.2026.571698.1375.
18. Alshlash M, Kitaz A, Abdelwahed W. (2023). Qualitative Phytochemical Screening, Antioxidant and Wound Healing Activities of *Pistacia Palaestina* Boiss. Extracts. Bull. Pharm. Sci. Assiut, 46, 83–96 https://doi.org /10.21608/bfsa.2023.300765.

19. Nurani LH, Kumalasari E, Zainab Z, Mursyidi A, Widyarini S, Rohman A. (2017). The determination of metal content, microbial contamination and dissolution assessment of the ethanol extract of *Pasak bumi* root. Pharmaciana, 7, 295 https://doi.org/10.12928/pharmaciana.v7i2.6751.
20. Nannipieri P, Ascher J, Ceccherini MT, Landi L, Pietramellara G, Renella G. (2003). Microbial diversity and soil functions,. 68(1):12-26DOI:10.1111/ejss.4_12398
21. Siddiqui FA, Bakshi V. (2025). Hydroalcoholic Extraction, Phytoconstituent Profiling by LC-HRMS, and Computational Analysis of *Lantana Camara* as Potential Glucokinase, Alpha Amylase, Alpha Glucosidase, and DPP-IV Inhibitors. Chem. Methodol., 9, 1189–220 https://doi.org/10.48309/chemm.2025.532981.1980.
22. Siddiqui FS. (2026). Computational Assessment of Secondary Metabolites as Potential Inhibitors of Methylenetetrahydrofolate Dehydrogenase-2 (MTHFD2). J. Phytopharm. Adv. Chem., 1, 3–17 https://doi.org /10.66220/wwze8340.
23. Pardaev J, Sadikova U. (2026). Computational Study of Alkaloids Targeting O-GlcNAc Transferase as Antidiabetic Agents. J. Phytopharm. Adv. Chem., 01, 18–29 https://doi.org/10.66220/qpba0t94.
24. Roy D, Roy D. (2026). Drug repurposing of some US FDA-approved drugs using Binding strength Studies for the Treatment of Methicillin- resistant *Staphylococcus aureus* Infection. J. Phytopharm. Adv. Chem., 01, 30–44 https://doi.org/10.66220/ecsrwe33.